arXiv:2409.03009v1 [hep-ex] 4 Sep 2024

Measurement of CP violation in $B^0 \to D^+ D^-$ and $B_s^0 \to D_s^+ D_s^-$ decays

LHCb collaboration[†]

Abstract

A time-dependent, flavour-tagged measurement of CP violation is performed with $B^0 \to D^+ D^-$ and $B_s^0 \to D_s^+ D_s^-$ decays, using data collected by the LHCb detector in proton-proton collisions at a centre-of-mass energy of 13 TeV corresponding to an integrated luminosity of $6\,\text{fb}^{-1}$. In $B^0 \to D^+ D^-$ decays the CP-violation parameters are measured to be

$$S_{D^+ D^-} = -0.552 \pm 0.100\,(\text{stat}) \pm 0.010\,(\text{syst}),$$
$$C_{D^+ D^-} = 0.128 \pm 0.103\,(\text{stat}) \pm 0.010\,(\text{syst}).$$

In $B_s^0 \to D_s^+ D_s^-$ decays the CP-violating parameter formulation in terms of ϕ_s and $|\lambda|$ results in

$$\phi_s = -0.086 \pm 0.106\,(\text{stat}) \pm 0.028\,(\text{syst})\,\text{rad},$$
$$|\lambda_{D_s^+ D_s^-}| = 1.145 \pm 0.126\,(\text{stat}) \pm 0.031\,(\text{syst}).$$

These results represent the most precise single measurement of the CP-violation parameters in their respective channels. For the first time in a single measurement, CP symmetry is observed to be violated in $B^0 \to D^+ D^-$ decays with a significance exceeding six standard deviations.

[†]Authors are listed at the end of this paper.

1 Introduction

Measurements of CP violation in $B^0_{(s)}$ mesons play a crucial role in the search for physics beyond the Standard Model (SM). With the increase in experimental precision, control over hadronic matrix elements becomes more important, which is a major challenge in most decay modes. In decays of beauty mesons to two charmed mesons $B \to DD$, this can be achieved by employing U-spin flavour symmetry and constraining the hadronic contributions by relating different CP-violation and branching fraction measurements [1–4].

The $B \to DD$ system gives access to a variety of interesting observables that probe elements of the Cabibbo–Kobayashi–Maskawa (CKM) quark-mixing matrix [5, 6]. In $B^0 \to D^+ D^-$ and $B^0_s \to D^+_s D^-_s$ decays, the CP-violating weak phases β and β_s can be measured, respectively. The phases arise in the interference between the B^0–$\overline{B}^0$ (B^0_s–$\overline{B}^0_s$) mixing and the tree-level decay amplitudes to the $D^+ D^-$ ($D^+_s D^-_s$) final state, leading to time-dependent CP asymmetries. The decays can also proceed through several other diagrams, as shown in Fig. 1. The CP asymmetries may arise from both SM contributions and new physics effects, if present.

In $B^0 \to D^+ D^-$ and $B^0_s \to D^+_s D^-_s$ decays, the same final state is accessible from both
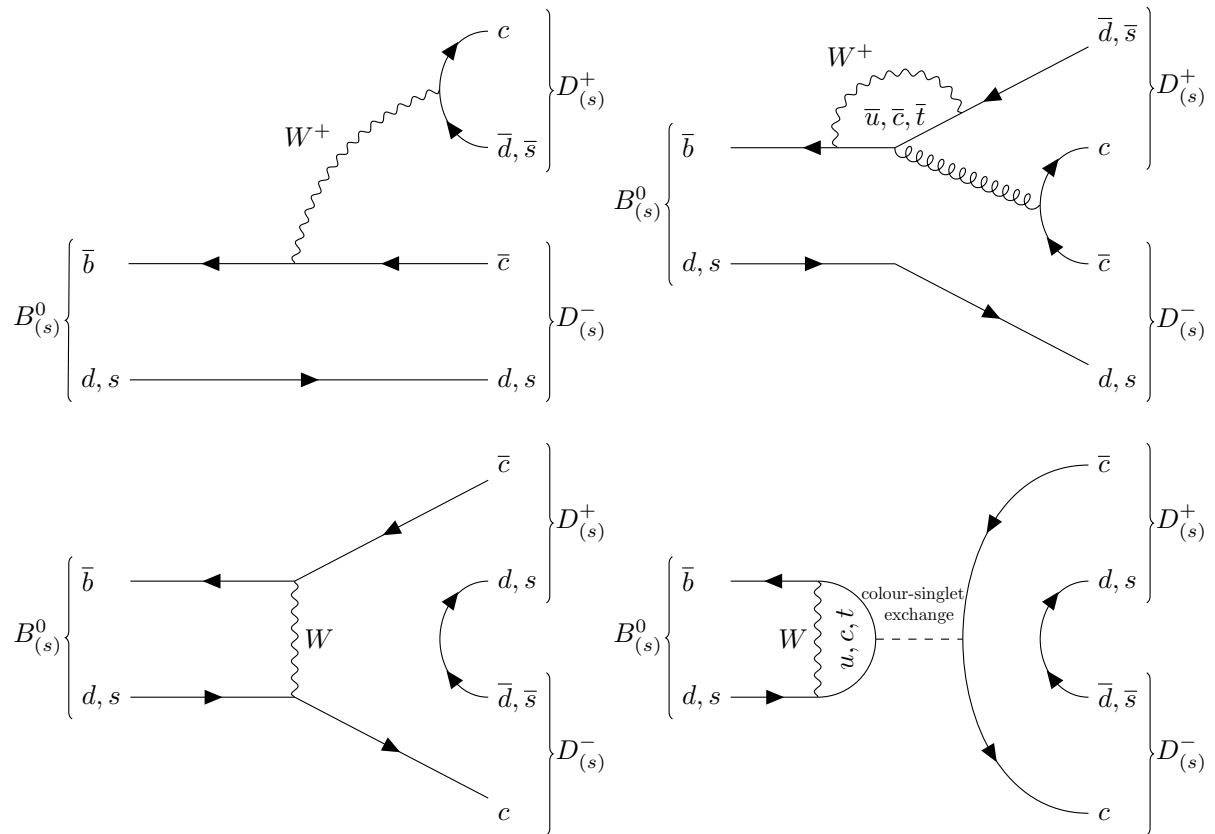

Figure 1: Dominant Feynman diagrams contributing to the $B^0 \to D^+ D^-$ and $B^0_s \to D^+_s D^-_s$ decays. The (top left) tree-level, (bottom left) exchange, (top right) penguin and (bottom right) penguin annihilation diagrams are shown.

$B^0_{(s)}$ and $\overline{B}^0_{(s)}$ states. The partial decay rate as a function of the decay time t is given by

$$\frac{\mathrm{d}\Gamma(t,d)}{\mathrm{d}t} \propto e^{-t/\tau_{B^0_{(s)}}} \left(\cosh \frac{\Delta\Gamma_q t}{2} + D_f \sinh \frac{\Delta\Gamma_q t}{2} + d\, C_f \cos \Delta m_q t - d\, S_f \sin \Delta m_q t \right), \quad (1)$$

where $\Delta\Gamma_q = \Gamma_{q\mathrm{L}} - \Gamma_{q\mathrm{H}}$ and $\Delta m_q = m_{q\mathrm{H}} - m_{q\mathrm{L}}$ are the decay-width difference and mass difference of the heavy and light B^0 ($q = d$) or B^0_s ($q = s$) mass eigenstates, $\tau_{B^0_{(s)}}$ is the mean lifetime of the $B^0_{(s)}$ meson and the tag d represents the flavour at production taking the value $+1$ for a $B^0_{(s)}$ meson and -1 for a $\overline{B}^0_{(s)}$ meson. The CP-violation parameters are defined as

$$D_f = -\frac{2|\lambda_f|\cos\phi_q}{1+|\lambda_f|^2}, \; C_f = \frac{1-|\lambda_f|^2}{1+|\lambda_f|^2}, \; S_f = -\frac{2|\lambda_f|\sin\phi_q}{1+|\lambda_f|^2},$$

$$\lambda_f = \frac{q}{p}\frac{\bar{A}_f}{A_f} \text{ and } \phi_q = -\arg\lambda_f, \quad (2)$$

where A_f and $\bar{A}_f$ are the decay amplitudes of $B^0_{(s)}$ and $\overline{B}^0_{(s)}$ to the common final state f and the ratio q/p describes mixing of the $B^0_{(s)}$ mesons. The parameter D_f cannot be measured in B^0 decays because, at the current experimental precision, $\Delta\Gamma_d$ is compatible with zero. Thus, the decay rates for $B^0 \to D^+D^-$ can be simplified to

$$\frac{\mathrm{d}\Gamma(t,d)}{\mathrm{d}t} \propto e^{-t/\tau_{B^0}} \left(1 + d\, C_{D^+D^-} \cos \Delta m_d t - d\, S_{D^+D^-} \sin \Delta m_d t\right). \quad (3)$$

If only tree-level contributions in $B^0 \to D^+D^-$ decays are considered, direct CP violation vanishes resulting in $C_{D^+D^-} = 0$ and $S_{D^+D^-} = -\sin\phi_d = -\sin 2\beta$. This assumption is valid within the current experimental precision for $B^0 \to J/\psi K^0_\mathrm{S}$ decays, where β can be measured with high precision as recently reported by LHCb [7]. However, in $B^0 \to D^+D^-$ measurements the loop-mediated penguin contributions shown in Fig. 1 cannot be neglected and an additional phase shift is measured via $\sin(2\beta + \Delta\phi_d) = -S_{D^+D^-}/\sqrt{1 - C^2_{D^+D^-}}$. This measurement enables higher-order corrections to the measurement of ϕ_s in $B^0_s \to D^+_s D^-_s$ decays to be constrained, under the assumption of U-spin flavour symmetry.

Due to the similarities of the two decay channels, a parallel measurement of the CP-violation parameters in $B^0 \to D^+D^-$ and $B^0_s \to D^+_s D^-_s$ decays is performed. Both decays have been previously studied by LHCb [8, 9], while measurements of the CP-violation parameters in $B^0 \to D^+D^-$ decays have been performed by BaBar [10] and Belle [11]. The Belle result lies outside the physically allowed region and shows a small tension with the other measurements.

This analysis uses proton-proton (pp) collision data collected by the LHCb experiment during the years 2015 to 2018 corresponding to an integrated luminosity of $6\,\mathrm{fb}^{-1}$. The $B^0 \to D^+D^-$ candidates are reconstructed through the decays $D^+ \to K^-\pi^+\pi^+$ and $D^+ \to K^-K^+\pi^+$.[1] These decays have the highest branching fractions into charged kaons and pions. Candidates where both $D^\pm$ mesons decay via $D^+ \to K^-K^+\pi^+$ are not considered due to the smaller branching fraction of this mode. Similarly, one of the $D^\pm_s$ mesons from the $B^0_s \to D^+_s D^-_s$ candidates is always reconstructed through the decay $D^+_s \to K^-K^+\pi^+$ and the other is reconstructed through the decays $D^+_s \to K^-K^+\pi^+$, $D^+_s \to \pi^-K^+\pi^+$ or $D^+_s \to \pi^-\pi^+\pi^+$.

---

[1] If not stated otherwise, charge-conjugated decays are implied.

Both signal channels and a dedicated $B^0 \to D_s^+ D^-$ control channel are selected by similar criteria with only minor differences as described in Sec. 3. A mass fit is performed separately for each final state to statistically subtract the remaining background as described in Sec. 4. The knowledge of the initial flavour of the candidates is crucial for measurements of time-dependent asymmetries in neutral B-meson decays. In Sec. 5 the algorithms used to determine the initial flavour of the $B^0_{(s)}$ mesons are described. The decay-time fit to measure the CP-violation parameters is described in Sec. 6 and the systematic uncertainties are discussed in Sec. 7. In Sec. 8 the results are presented from both this analysis and in combination with previous LHCb measurements.

2 Detector and simulation

The LHCb detector [12, 13] is a single-arm forward spectrometer covering the pseudorapidity range $2 < \eta < 5$, designed for the study of particles containing b or c quarks. The detector includes a high-precision tracking system consisting of a silicon-strip vertex detector surrounding the pp interaction region [14], a large-area silicon-strip detector located upstream of a dipole magnet with a bending power of about $4\,\mathrm{T\,m}$, and three stations of silicon-strip detectors and straw drift tubes [15] placed downstream of the magnet. The tracking system provides a measurement of the momentum, p, of charged particles with a relative uncertainty that varies from 0.5% at low momentum to 1.0% at $200\,\mathrm{GeV}/c$. The minimum distance of a track to a primary pp collision vertex (PV), the impact parameter (IP), is measured with a resolution of $(15 + 29/p_\mathrm{T})\,\upmu\mathrm{m}$, where p_T is the component of the momentum transverse to the beam, in GeV/c. Different types of charged hadrons are distinguished using information from two ring-imaging Cherenkov detectors [16]. Photons, electrons and hadrons are identified by a calorimeter system consisting of scintillating-pad and preshower detectors, an electromagnetic and a hadronic calorimeter. Muons are identified by a system composed of alternating layers of iron and multiwire proportional chambers [17].

Simulation is required to model the effects of the detector acceptance and the imposed selection requirements. Samples of signal decays are used to determine the parameterisation of the signal mass distributions and decay-time resolution model. In the simulation, pp collisions are generated using PYTHIA [18] with a specific LHCb configuration [19]. Decays of unstable particles are described by EVTGEN [20], in which final-state radiation is generated using PHOTOS [21]. The interaction of the generated particles with the detector, and its response, are implemented using the GEANT4 toolkit [22] as described in Ref. [23]. The underlying pp interaction is reused multiple times, with an independently generated signal decay for each [24]. To account for differences between the distributions of particle identification (PID) variables in simulation and data, the PIDCalib package [25] is used to reweight the distributions in the simulation.

3 Selection

The online event selection is performed by a trigger [26], which consists of a hardware stage based on information from the calorimeter and muon systems, followed by a software stage which applies a full event reconstruction. At the hardware trigger stage, events are required to have a muon with high p_T or a hadron, photon or electron with high transverse

energy in the calorimeters. The software trigger requires a two-, three- or four-track secondary vertex with a significant displacement from any primary pp interaction vertex. At least one charged particle must have a transverse momentum $p_T > 1.6\,\text{GeV}/c$ and be inconsistent with originating from a PV. A multivariate algorithm [27, 28] is used for the identification of secondary vertices consistent with the decay of a b hadron.

In the offline selection, $D^{\pm}$ and $D_s^{\pm}$ candidates are reconstructed through their decays into the selected final-state particles, which are required to satisfy loose selection criteria on their momentum, transverse momentum and PID variables, and be inconsistent with originating from any PV. The $D^{\pm}$ and $D_s^{\pm}$ candidates should form vertices with a good fit quality and the scalar sum of transverse momenta of their three final-state particles should be greater than $1800\,\text{MeV}/c$. All possible combinations of tracks forming a common vertex should have a distance of closest approach smaller than $0.5\,\text{mm}$. The $B_{(s)}^0$ candidates are reconstructed from two $D^{\pm}$ or $D_s^{\pm}$ candidates with opposite charges that form a good-quality vertex. The momentum vector of the $B_{(s)}^0$ candidates should point from the PV to the secondary vertex. The scalar sum of the transverse momenta of all six final-state particles is required to be greater than $5000\,\text{MeV}/c$. The invariant masses of the $D^{\pm}$ and $D_s^{\pm}$ candidates are required to be within a window of $\pm 45\,\text{MeV}/c^2$ around their known values [29]. This requirement, of about ± 4 times the mass resolution, retains almost all candidates while separating the $D^{\pm}$ from the $D_s^{\pm}$ mass region. To suppress single-charm decays of the form $B_{(s)}^0 \to D_{(s)}^+ h^+ h^- h^-$, both $D_{(s)}^+$ candidates are required to have a significant flight distance from the $B_{(s)}^0$ decay vertex.

In the reconstruction of the $D_{(s)}^+$ candidates, background contributions can arise from the misidentification of the final-state particles. Misidentification from a pion, kaon or proton is considered. The three-body invariant masses are recomputed to identify background decays from D^+, D_s^+ and Λ_c^+ states. The masses for potential two-body background contributions arising from intermediate ϕ and D^0 decays are similarly computed. These background sources are suppressed by PID requirements within the mass windows of the known particle masses.

A particularly challenging background arises from the misidentification between $D^+ \to K^- \pi^+ \pi^+$ and $D_s^+ \to K^- K^+ \pi^+$ decays. The $\pi^+ \leftrightarrow K^+$ misidentification shifts the mass region of the reconstructed D^+ candidates to that of the D_s^+ or vice versa. In this case, a simple PID requirement does not provide the necessary rejection of the particularly large background contribution from $B^0 \to D_s^+ D^-$ decays. To distinguish between the two decays a boosted decision tree (BDT) algorithm is trained utilising the `xgboost` module from the `scikit-learn` package [30]. Simulated D^+ and D_s^+ decays from the $B^0 \to D^+ D^-$, $B^0 \to D_s^+ D^-$ and $B_s^0 \to D_s^+ D_s^-$ samples are used to train the BDT classifier. A k-folding procedure with $k = 5$ is used to avoid overtraining [31]. Various two- and three-body invariant masses, recomputed with different final-state particle hypotheses, are used in the training. Additionally, the flight distance of the $D_{(s)}^+$ candidates, and the PID variables of those particles that are potentially misidentified, are used. The requirements on the BDT-classifier output are chosen to suppress the D_s^+ candidates in the $B^0 \to D^+ D^-$ channel and D^+ candidates in the $B_s^0 \to D_s^+ D_s^-$ channel to negligible levels. This is verified by applying the requirements to the simulated samples, which results in the rejection of more than 99% of the respective candidates.

A second BDT classifier is trained to suppress combinatorial background. As a signal proxy, all available simulated $B^0 \to D^+ D^-$, $B^0 \to D_s^+ D^-$ and $B_s^0 \to D_s^+ D_s^-$ samples are

used while the background proxy is taken from the upper-mass sideband of the data, which is defined as $m_{D_{(s)}^+ D_{(s)}^-} > 5600\,\text{MeV}/c^2$, beyond the $B_{(s)}^0$-candidate mass fit region. The variables used in the training are all transverse momenta of intermediate and final-state particles; the flight distance and the difference in invariant mass from the known value [29] of the $D_{(s)}^+$ candidates; the angle between the $D_{(s)}^+$ flight direction and each of the decay products; the χ_{IP}^2 of the $B_{(s)}^0$ and $D_{(s)}^+$ candidates, which is the difference in the χ^2 value of the PV fit with and without the particle being considered in the calculation. Similar to the strategy used in Ref. [32], the requirement on the BDT-classifier output is chosen to minimise the uncertainties on the CP-violation parameters.

The invariant mass used in the mass fits is computed from a kinematic fit to the decay chain with constraints on all charm-meson masses to improve the invariant-mass resolution of the $B_{(s)}^0$ candidates [33]. For calculation of the decay time, a constraint on the PV is used in the kinematic fit. To avoid correlations between the decay time and the invariant mass, no constraints on the charm-masses are used.

Contributions from partially reconstructed backgrounds are reduced to negligible levels by restricting the invariant mass of the B^0 candidates to lie within the range 5240–5540 MeV/c^2. The decay-time range is chosen to be 0.3–10.3 ps, where the lower boundary is set to reduce background originating from the PV. For B_s^0 candidates the same decay-time range is chosen, but the invariant-mass range is 5300–5600 MeV/c^2.

After the selection, multiple candidates are found in about 1% of the events. Usually, these candidates differ in just one track or PID assignment. Since it is very unlikely to find two genuine candidates in one event, only one of the candidates is chosen arbitrarily.

4 Mass fit

An extended unbinned maximum-likelihood fit to the invariant mass of the $B_{(s)}^0$ candidates is performed to extract per-event weights via the *sPlot* technique [34]. These weights are used in the decay-time fit to statistically subtract the background. Pseudoexperiment studies indicate that any residual correlation between the decay time and the mass introduces no meaningful bias into the CP-violation measurement.

The mass model in the $B^0 \to D^+ D^-$ channel consists of a signal component and two background components to model $B_s^0 \to D^+ D^-$ decays and the combinatorial background. A double-sided Hypatia probability density function (PDF) [35] is used to model the signal component. The shape parameters are determined by a fit to simulated $B^0 \to D^+ D^-$ decays and fixed in the fit to data, while the peak position and width of the distribution are allowed to vary. The same model is used for the $B_s^0 \to D^+ D^-$ component with a shift of the peak position by the known mass difference between the B^0 and B_s^0 mesons [29]. An exponential PDF is used to model the combinatorial background.

The mass model in the $B_s^0 \to D_s^+ D_s^-$ channel consists only of a signal component and a combinatorial background component, which are parameterised as in the $B^0 \to D^+ D^-$ fit. Mass fits are performed separately for each final state. Figures 2 and 3 show the results of the fits to all $B^0 \to D^+ D^-$ and $B_s^0 \to D_s^+ D_s^-$ final states, respectively. The fits yield an overall number of $5\,695 \pm 100$ $B^0 \to D^+ D^-$ and $13\,313 \pm 135$ $B_s^0 \to D_s^+ D_s^-$ signal decays.

Figure 2: Invariant-mass distribution of $B^0 \to D^+D^-$ decays. The data are shown as points and the full PDF is shown as a solid-blue line for (left) both $D^\pm$ candidates decaying through $D^+ \to K^-\pi^+\pi^+$ and (right) one $D^\pm$ candidate decaying through $D^+ \to K^-K^+\pi^+$.
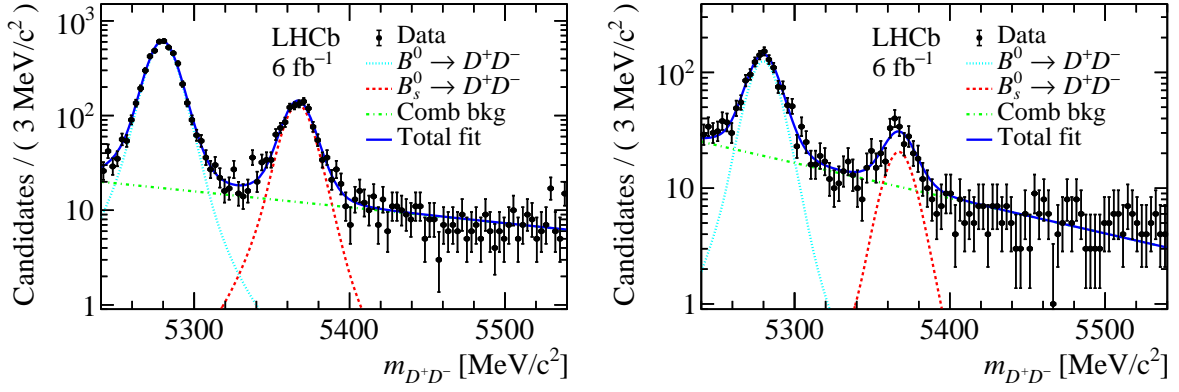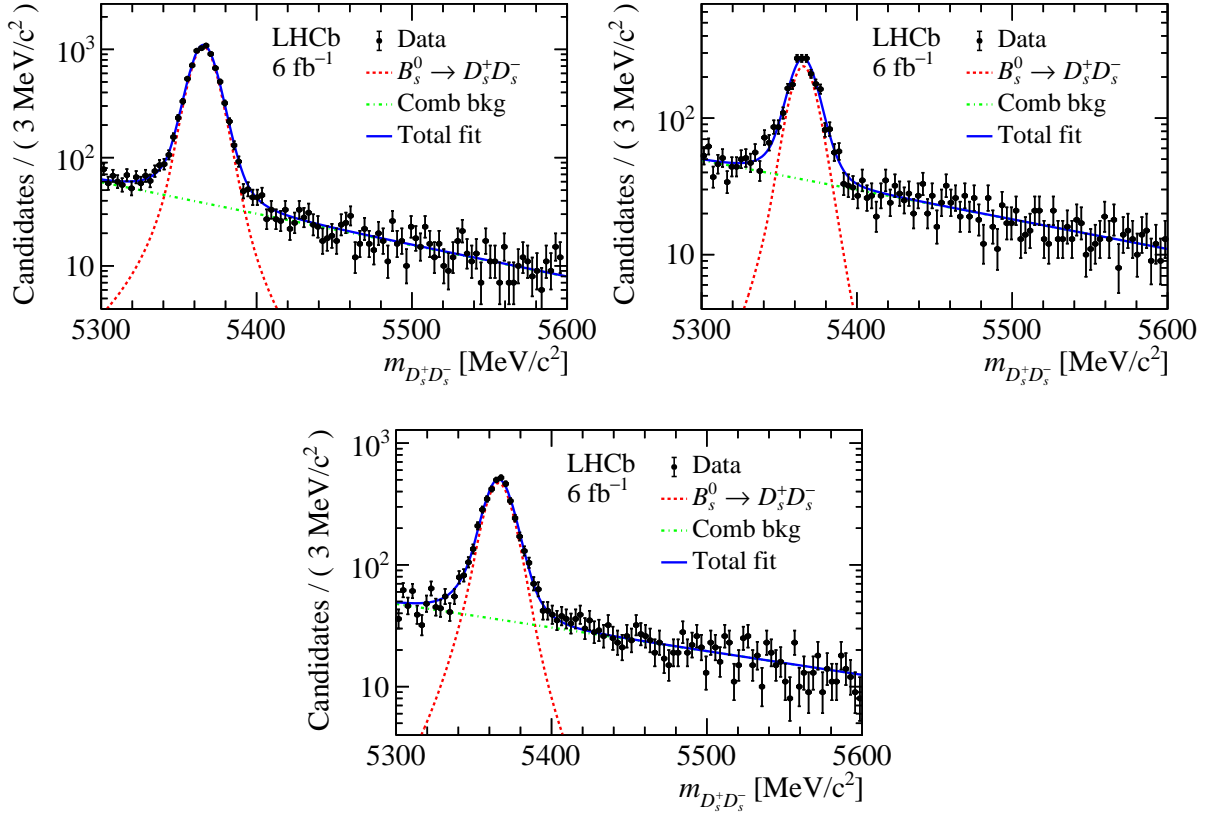

Figure 3: Invariant-mass distribution of $B_s^0 \to D_s^+D_s^-$ decays. The data are shown as points and the full PDF is shown as a solid-blue line for (left) both $D_s^\pm$ candidates decaying through $D_s^+ \to K^-K^+\pi^+$, (right) one $D_s^\pm$ candidate decaying through $D_s^+ \to \pi^-K^+\pi^+$ and (bottom) one $D_s^\pm$ candidate decaying through $D_s^+ \to \pi^-\pi^+\pi^+$.

5 Flavour tagging

For time-dependent CP violation measurements of neutral B mesons, the flavour of the meson at production is required. At LHCb the method used to determine the initial flavour is called flavour tagging. These algorithms exploit the fact that in pp collisions, b and $\bar{b}$ quarks are almost exclusively produced in pairs. When the b quark forms a $\overline{B}$ meson (and similarly the $\bar{b}$ quark forms a B meson), additional particles are produced in the fragmentation process. From the charges and types of these particles, the flavour of the signal B meson at production can be inferred. The tagging algorithm that uses charged pions or protons from the fragmentation process of the b quark that leads to the $\overline{B}^0$ signal is called the same-side (SS) tagger [36]. In the case of signal $\overline{B}_s^0$ mesons, charged kaons are used by the SS tagger [37]. The opposite-side (OS) tagger uses information from electrons and muons from semileptonic b decays, kaons from the $b \to c \to s$ decay chain, secondary charm hadrons and the charges of tracks from the secondary vertex of the other b-hadron decay [38, 39]. Each algorithm i provides individual tag decisions, d_i, and a predicted mistag, η_i, which is an estimate of the probability that the tag decision is wrong. The tag decision takes the values -1 for a $\overline{B}$ meson, 1 for a B meson and 0 if no tag decision can be made. The predicted mistag ranges from 0 to 0.5 and takes the value of 0.5 for untagged events. Each predicted mistag distribution is given by the output of a BDT that is trained on flavour-specific decays [40] and has to be calibrated to represent the mistag probability, $\omega_i(\eta_i)$, in the signal decay. Flavour-specific control channels with kinematics similar to the signal are used to obtain a calibration curve. This is found to be well-described by a linear function. Following calibration, the individual taggers are combined separately for OS and SS cases, and the resulting mistag distributions are recalibrated. These calibrations are used in the decay-time fit to determine the CP-violation parameters to which the uncertainties on the calibration parameters are propagated through means of a Gaussian constraint.

To calibrate the SS and OS taggers of the $B^0 \to D^+ D^-$ channel, as well as the OS tagger of the $B_s^0 \to D_s^+ D_s^-$ channel, $B^0 \to D_s^+ D^-$ decays are used. These have very similar kinematics to the signal decays and the selection is very similar, as described in Sec. 3. The SS kaon tagger used for $B_s^0 \to D_s^+ D_s^-$ decays is calibrated with the $B_s^0 \to D_s^- \pi^+$ channel. A reweighting process is applied to ensure the calibration sample matches the distributions of the signal channel in the transverse momentum of the B_s^0 meson, the pseudorapidity, the number of tracks and the number of PVs. Additionally, the compatibility of the calibration between $B_s^0 \to D_s^- \pi^+$ and $B_s^0 \to D_s^+ D_s^-$ decays is verified by comparing the calibration parameters determined using simulation.

The performance of the tagging algorithms is measured by the tagging power $\epsilon_{\mathrm{tag}} D^2$, where ϵ_{tag} is the fraction of tagged candidates and $D = 1 - 2\omega$ is the dilution factor introduced by the mistag probability, ω. The tagging power is a statistical dilution factor due to imperfect tagging, equivalent to an efficiency with respect to a sample with perfect tagging. Overall tagging powers of $(6.28 \pm 0.11)\%$ in $B^0 \to D^+ D^-$ and $(5.60 \pm 0.07)\%$ in $B_s^0 \to D_s^+ D_s^-$ decays are achieved.

6 Decay-time fit

An unbinned maximum-likelihood fit to the signal-weighted decay-time distribution is performed to determine the *CP*-violation parameters. In order to avoid experimenter bias, the values of the *CP*-violation parameters were not examined until the full procedure had been finalised.

The measured decay-time distribution of the $B^0_{(s)}$ candidates given the tag decisions $\vec{d} = (d_{\mathrm{OS}}, d_{\mathrm{SS}})$ and predicted mistags $\vec{\eta} = (\eta_{\mathrm{OS}}, \eta_{\mathrm{SS}})$ is described by the PDF

$$\mathcal{P}(t, \vec{d} \,|\, \vec{\eta}) = \epsilon(t) \cdot \left(\mathcal{B}(t', \vec{d} \,|\, \vec{\eta}) \otimes \mathcal{R}(t - t') \right), \tag{4}$$

where $\mathcal{B}(t', \vec{d} \,|\, \vec{\eta})$ describes the distribution of the true decay time t', which is convolved with the decay-time resolution function $\mathcal{R}(t - t')$, and the acceptance function $\epsilon(t)$ describes the total efficiency as a function of the reconstructed decay time. The PDF describing the decay-time distribution can be deduced from Eq. (1) and takes the general form

$$
\begin{aligned}
\mathcal{B}(t', \vec{d} \,|\, \vec{\eta}) \propto e^{-t'/\tau} \bigg(& C^{\mathrm{eff}}_{\cosh}(\vec{d} \,|\, \vec{\eta}) \cosh \frac{\Delta\Gamma_q t'}{2} + C^{\mathrm{eff}}_{\sinh}(\vec{d} \,|\, \vec{\eta}) \sinh \frac{\Delta\Gamma_q t'}{2} \\
& - C^{\mathrm{eff}}_{\cos}(\vec{d} \,|\, \vec{\eta}) \cos \Delta m_q t' + C^{\mathrm{eff}}_{\sin}(\vec{d} \,|\, \vec{\eta}) \sin \Delta m_q t' \bigg).
\end{aligned}
\tag{5}
$$

The effective coefficients are given by

$$
\begin{aligned}
C^{\mathrm{eff}}_{\cosh} &= \Sigma(\vec{d} \,|\, \vec{\eta}) + A_{\mathrm{prod}} \Delta(\vec{d} \,|\, \vec{\eta}), & C^{\mathrm{eff}}_{\cos} &= C_f \left(\Delta(\vec{d} \,|\, \vec{\eta}) + A_{\mathrm{prod}} \Sigma(\vec{d} \,|\, \vec{\eta}) \right), \\
C^{\mathrm{eff}}_{\sinh} &= D_f \left(\Sigma(\vec{d} \,|\, \vec{\eta}) + A_{\mathrm{prod}} \Delta(\vec{d} \,|\, \vec{\eta}) \right), & C^{\mathrm{eff}}_{\sin} &= S_f \left(\Delta(\vec{d} \,|\, \vec{\eta}) + A_{\mathrm{prod}} \Sigma(\vec{d} \,|\, \vec{\eta}) \right),
\end{aligned}
\tag{6}
$$

where the production asymmetry $A_{\mathrm{prod}} = (N_{\overline{B}^0_{(s)}} - N_{B^0_{(s)}})/(N_{\overline{B}^0_{(s)}} + N_{B^0_{(s)}})$ represents the difference in the production rates of $\overline{B}^0_{(s)}$ and $B^0_{(s)}$ mesons. The functions

$$
\begin{aligned}
\Sigma(\vec{d}, \vec{\eta}) &= P(\vec{d}, \vec{\eta} | \overline{B}^0_{(s)}) + P(\vec{d}, \vec{\eta} | B^0_{(s)}) \text{ and} \\
\Delta(\vec{d}, \vec{\eta}) &= P(\vec{d}, \vec{\eta} | \overline{B}^0_{(s)}) - P(\vec{d}, \vec{\eta} | B^0_{(s)})
\end{aligned}
\tag{7}
$$

are dependent on the tagging calibration parameters, where $P(\vec{d}, \vec{\eta} | B^0_{(s)})$ and $P(\vec{d}, \vec{\eta} | \overline{B}^0_{(s)})$ are the probabilities of observing the tagging decisions $\vec{d}$ and the predicted mistags $\vec{\eta}$, given the true flavour $B^0_{(s)}$ or $\overline{B}^0_{(s)}$, respectively.

$B^0 \to D^+ D^-$

The decay-time fit of $B^0 \to D^+ D^-$ decays is insensitive to $C^{\mathrm{eff}}_{\sinh}$ under the assumption that $\Delta\Gamma_d$ is zero. Moreover, due to the long oscillation period of the B^0 mesons, the decay-time resolution of around 52 fs has a very small impact on the *CP*-violation parameters. The decay-time resolution model consists of three Gaussian functions that have a common mean and different widths. The parameters of the model are determined from simulation and fixed in the fit to data.
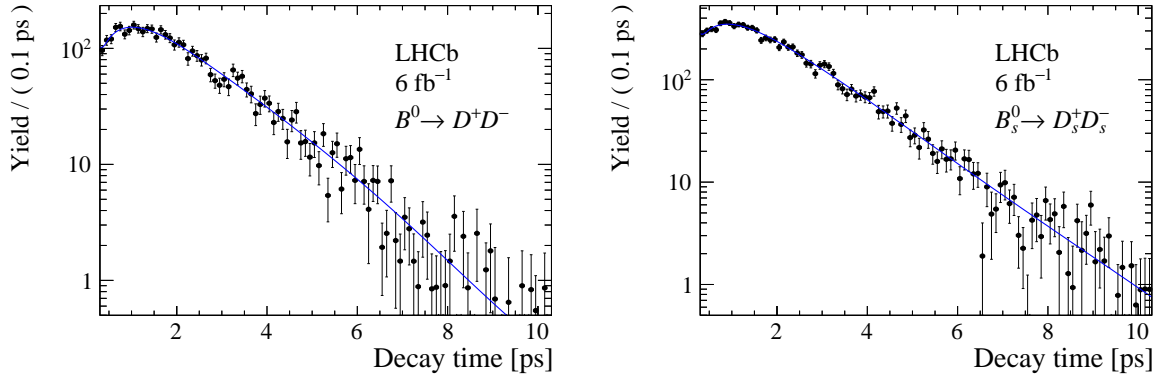
Figure 4: Decay-time distribution of (left) $B^0 \to D^+ D^-$ and (right) $B^0_s \to D^+_s D^-_s$ candidates. The background-subtracted data are shown as points and the projection of the PDF is shown as a solid blue line.

The selection and reconstruction efficiency depends on the B^0 decay time due to displacement requirements made on the final-state particles and a decrease in the reconstruction efficiency for tracks with large impact parameter with respect to the beamline [41]. The decay-time dependent efficiency is modeled by cubic-spline functions [42] with five knots at $(0.3, 0.5, 2.7, 6.3, 10.3)$ ps, whose positions were determined using simulation. The spline coefficients are free to vary in the fit.

Gaussian constraints are used to account for the uncertainties on the tagging calibration parameters, the B^0 lifetime, the oscillation frequency, Δm_d, and the production asymmetry. The world-average values are used for the external parameters [43], while the production asymmetry is taken from a similar time-dependent analysis of $B^0 \to D^{*\pm} D^{\mp}$ decays [44]. The tagging efficiencies are free to vary in the decay-time fit. Figure 4 (left) shows the results of the decay-time fit for this channel.

$B^0_s \to D^+_s D^-_s$

In the decay-time fit of $B^0_s \to D^+_s D^-_s$ decays, the hyperbolic terms of Eq. (5) can be measured provided that $\Delta\Gamma_s$ is not zero. Moreover, the definitions from Eq. (2) are used to directly determine the parameters ϕ_s and $|\lambda|$. The acceptance function, the tagging parameters and external parameters are treated in the same way as for the $B^0 \to D^+ D^-$ decays. In addition to the lifetime and the oscillation frequency, Δm_s, the decay-width difference $\Delta\Gamma_s$ is constrained in the fit to the world-average value [43]. The value of the production asymmetry is taken from the control channel $B^0_s \to D^-_s \pi^+$ as described in Ref. [45].

Due to the high oscillation frequency of the B^0_s meson, the decay-time resolution plays an important role. A per-event decay-time resolution is determined based on the per-event decay-time uncertainty estimated from the vertex fit, which is calibrated using a sample of $D^-_s \pi^+$ candidates, with $D^-_s \to \phi(K^+ K^-)\pi^-$, and additional requirements imposed to suppress candidates produced in B decays to negligible levels. The measured decay time of the remaining candidates, which originate from the PV, is consistent with zero, and their distribution is used to assess resolution and bias effects. A linear fit to the measured and
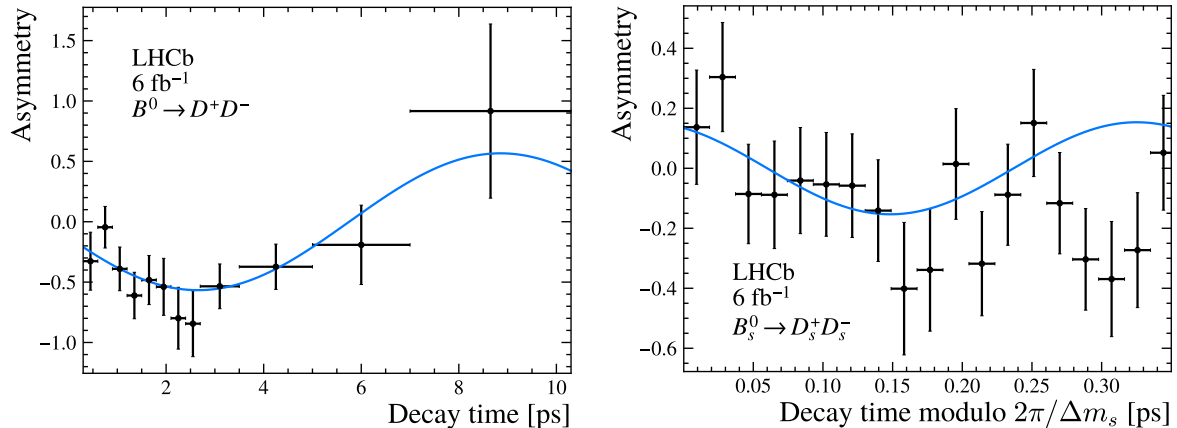
Figure 5: Decay-time-dependent CP asymmetry of (left) $B^0 \to D^+D^-$ and (right) $B_s^0 \to D_s^+D_s^-$ candidates. The asymmetry in the background-subtracted data is shown as points and the projection of the PDF is shown as a solid blue line. Due to the high oscillation frequency of the B_s^0 mesons, the corresponding distribution is folded onto one oscillation period.

predicted decay-time resolution is performed. A scale factor is then applied to translate the resulting calibration to the signal $B_s^0 \to D_s^+D_s^-$ mode. It is determined by comparing the decay-time resolution of $B_s^0 \to D_s^-\pi^+$ and $B_s^0 \to D_s^+D_s^-$ decays in simulation. Figure 4 (right) shows the results of the decay-time fit for this channel.

The decay-time-dependent CP asymmetry and the projection of the PDF are shown in Fig. 5 for (left) $B^0 \to D^+D^-$ and (right) $B_s^0 \to D_s^+D_s^-$ decays. The CP asymmetry in each decay-time bin is given by $A^{CP} = -(\sum_j w_j d_j D_j)/(\sum_j w_j D_j^2)$ with the tagging decision d_j, the tagging dilution D_j and the signal weight w_j obtained by the $sPlot$ method [7], for each candidate j.

7 Systematic uncertainties and cross-checks

A variety of cross-checks are performed and potential sources of systematic uncertainties are considered.

The decay-time fit is performed on a simulated $B^0 \to D^+D^-$ sample using the same strategy for the tagging calibration as for the fit to data. A second fit is performed where instead of the reconstructed tagging, the truth information of the initial flavour of the B^0 mesons is used. Both results of the CP-violation parameters agree with the generated values.

The decay-time fit is performed on several subsets of the data to test the consistency of the results. The data subdivision is done according to the final state, magnet polarity, years of data taking and tagging information (OS only or SS only). Consistent results are found in all cases.

A bootstrapping procedure [46] is used to cross-check the statistical uncertainty from the decay-time fit to data. A data set is created by randomly drawing candidates from the original sample until a certain number of candidates is reached that itself is drawn from a Poisson distribution with the expected number of candidates matching the original

data sample. This entails that the same candidate can be drawn multiple times. The mass and decay-time fits are performed on this data set to first statistically subtract the background and then determine the CP-violation parameters. The residual of the fit result with respect to the baseline fit is stored and the whole procedure is repeated until the distribution of the residuals is not significantly affected by statistical fluctuations. The statistical uncertainties from the fits to data are shown to be accurate as they are consistent with the standard deviations of the residuals, and the correlation coefficients lie within expectations.

A decay-time fit with a different set of knots for the acceptance function is performed. The difference in the results with respect to the baseline fit is assigned as a systematic uncertainty.

To test the fit strategy, pseudoexperiments are performed. In each pseudoexperiment, the mass and decay time are generated using the results of the baseline fit to data. The background contributions are generated with a specific time dependence, assuming CP symmetry for the $B_s^0 \to D^+ D^-$ background. Similar to the bootstrapping procedure, the baseline fitting procedure is performed on the pseudoexperiments and the residuals are collected. For $B^0 \to D^+ D^-$ decays, the mean values of the results are found to be consistent with the input values within the statistical uncertainties, while the fits to the $B_s^0 \to D_s^+ D_s^-$ pseudoexperiments show a small bias of -0.002 in ϕ_s and 0.008 in $|\lambda_{D_s^+ D_s^-}|$. This is of the order of a few percent of the statistical uncertainty and is subtracted from the biases found in the following studies.

The following systematic uncertainties are determined using the same procedure, with the only difference being that an alternative model is used to generate pseudoexperiments in each case. A bias in the distribution of the residuals is assigned as a systematic uncertainty.

The sum of two Crystal Ball functions [47], with parameters obtained from a fit to simulation, is used in the pseudoexperiments to test the choice of the signal mass model.

Since $\Delta\Gamma_d$ is fixed to zero in the decay-time fit of $B^0 \to D^+ D^-$ decays, a systematic uncertainty is assigned for this assumption. The value of $\Delta\Gamma_d$ is varied in the pseudo-experiments from the assumed value of zero by $\pm 1\sigma$, where σ is the uncertainty of the world average value of $\Delta\Gamma_d$ [29]. The value of $D_{D^+ D^-}$ is calculated from the normalisation condition $D_{D^+ D^-} = \pm\sqrt{1 - S_{D^+ D^-}^2 - C_{D^+ D^-}^2}$ and the largest deviation is assigned as the systematic uncertainty.

In the $B^0 \to D^+ D^-$ channel the decay-time-resolution model is determined on simulation. Due to differences between simulation and data the resolution could be underestimated. The effect of underestimating the resolution is tested by increasing the width of the resolution function by 10% in the pseudoexperiments, which corresponds to the level measured in the B_s^0 system. It is found to be small and no further studies are considered.

In the $B_s^0 \to D_s^+ D_s^-$ channel, $D_s^- \pi^+$ candidates originating from the PV are used to determine a per-event resolution calibration. Only $D_s^- \to \phi(K^+ K^-)\pi^-$ decays are used and assumed to represent the resolution of the whole sample. A second calibration is obtained using a sample of $D_s^- \to K^+ K^- \pi^-$ decays without specific requirements on the intermediate decays and used in the pseudoexperiments to assign a systematic uncertainty.

A decay-time bias caused by the misalignment of the vertex detector was observed in other LHCb analyses of data taken during the same period [7, 45] and confirmed in the present analysis. Due to the low oscillation frequency of B^0 mesons, this has a negligible effect on the measurement of the CP-violation parameters, as shown in Ref. [45] and so

Table 1: Systematic uncertainties for the $B^0 \to D^+D^-$ and $B_s^0 \to D_s^+D_s^-$ channel. A dash (—) is used to denote that a systematic has not been evaluated. The total systematic uncertainty is the quadratic sum of the individual uncertainties.

Source	$S_{D^+D^-}$	$C_{D^+D^-}$	$\phi_s\,[\mathrm{rad}]$	$|\lambda_{D_s^+D_s^-}|$
Mass model	0.001	0.005	0.003	0.005
$\Delta\Gamma$	0.010	0.005	—	—
Decay-time resolution	0.002	0.007	0.011	0.027
Decay-time bias	—	—	0.026	0.014
Acceptance function	0.001	0.001	< 0.001	0.001
Total	0.010	0.010	0.028	0.031

is not evaluated here. However, in B_s^0 decays, this bias could have a significant impact on the measurement. To evaluate the effect, the mean of the resolution function in the generation of the pseudoexperiments is set to the largest observed bias.

The individual systematic uncertainties on the CP-violation parameters are reported in Table 1 and summed in quadrature.

8   Results and interpretation

A flavour-tagged time-dependent analysis of $B^0 \to D^+D^-$ and $B_s^0 \to D_s^+D_s^-$ decays is performed using proton-proton collision data collected by the LHCb experiment during the years 2015 to 2018, corresponding to an integrated luminosity of $6\,\mathrm{fb}^{-1}$. Approximately $5\,700\ B^0 \to D^+D^-$ signal candidates are observed. A fit to their decay-time distribution, including evaluation of systematic uncertainties, gives the final results

$$S_{D^+D^-} = -0.552 \pm 0.100\,(\mathrm{stat}) \pm 0.010\,(\mathrm{syst}),$$
$$C_{D^+D^-} = \quad 0.128 \pm 0.103\,(\mathrm{stat}) \pm 0.010\,(\mathrm{syst}),$$

with a statistical correlation between the two parameters of $\rho(S_{D^+D^-}, C_{D^+D^-}) = 0.472$. The results and correlations of the external parameters from the decay-time fit are presented in Appendix A. Wilks' theorem [48] is used to determine the significance of the result, excluding systematic uncertainties. The hypothesis of CP symmetry, corresponding to $S_{D^+D^-} = C_{D^+D^-} = 0$, can be rejected by more than six standard deviations. The values are consistent with previous results from LHCb and BaBar [10], which correspond to a small contribution from higher-order SM corrections. Thus, this measurement will move the world average further away from the Belle measurement, which lies outside the physical region [11].

The result is combined with the previous LHCb measurement in this channel [8]. Due to the small effect of the external parameters on the result, the two measurements are assumed to be uncorrelated and the combined values are

$$S_{D^+D^-} = -0.549 \pm 0.085\,(\mathrm{stat}) \pm 0.015\,(\mathrm{syst}),$$
$$C_{D^+D^-} = \quad 0.162 \pm 0.088\,(\mathrm{stat}) \pm 0.009\,(\mathrm{syst}),$$

with a statistical correlation between the two parameters of $\rho(S_{D^+D^-}, C_{D^+D^-}) = 0.474$.

Approximately $13\,000$ $B_s^0 \to D_s^+ D_s^-$ signal candidates are observed and the final results of the decay-time fit and the systematic uncertainties are

$$\phi_s = -0.086 \pm 0.106\,(\text{stat}) \pm 0.028\,(\text{syst})\,\text{rad},$$
$$|\lambda_{D_s^+ D_s^-}| = 1.145 \pm 0.126\,(\text{stat}) \pm 0.031\,(\text{syst}),$$

with a statistical correlation between the two parameters of $\rho(\phi_s, |\lambda_{D_s^+ D_s^-}|) = -0.007$. Further information on the results of the decay-time fit is shown in Appendix A. This result is consistent with, and more precise than, the previous LHCb measurement [9]. The combination with the previous LHCb measurement, following the same strategy as for the $B^0 \to D^+ D^-$ decays, yields the values

$$\phi_s = -0.055 \pm 0.090\,(\text{stat}) \pm 0.021\,(\text{syst})\,\text{rad},$$
$$|\lambda_{D_s^+ D_s^-}| = 1.054 \pm 0.099\,(\text{stat}) \pm 0.020\,(\text{syst}),$$

with a statistical correlation between the two parameters of $\rho(\phi_s, |\lambda_{D_s^+ D_s^-}|) = 0.005$. The values are consistent with CP symmetry in the $B_s^0 \to D_s^+ D_s^-$ channel.

These results can be used in combination with other $B \to DD$ measurements to perform a global analysis and extract SM parameters as has previously been performed in Ref. [3]. They represent the most precise single measurements of the CP-violation parameters in their respective channels and the combined results supersede the previous LHCb measurements. For the first time, CP symmetry can be excluded by more than six standard deviations in a single measurement of $B^0 \to D^+ D^-$ decays.

Acknowledgements

Appendices

A   Results and correlations of external parameters

Table 2: Results of the external parameters from the decay-time fit to $B^0 \to D^+D^-$ data.

Parameter	Input value	Fit result
$\Delta m_d \, [\,\mathrm{ps}^{-1}\,]$	0.5065 ± 0.0019	0.5065 ± 0.0019
$\tau_{B^0} \, [\,\mathrm{ps}\,]$	1.519 ± 0.004	1.519 ± 0.004

Table 3: Correlation matrix of the CP parameters and the external parameters from the decay-time fit to $B^0 \to D^+D^-$ data.

	$S_{D^+D^-}$	$C_{D^+D^-}$	Δm_d	τ_{B^0}
$S_{D^+D^-}$	1.000	0.472	-0.014	< 0.001
$C_{D^+D^-}$		1.000	-0.022	< 0.001
Δm_d			1.000	< 0.001
τ_{B^0}				1.000

Table 4: Results of the external parameters from the decay-time fit to $B^0_s \to D^+_s D^-_s$ data.

Parameter	Input value	Fit result
$\Delta \Gamma_s \, [\,\mathrm{ps}^{-1}\,]$	0.083 ± 0.005	0.083 ± 0.005
$\Delta m_s \, [\,\mathrm{ps}^{-1}\,]$	17.765 ± 0.006	17.765 ± 0.006
$\tau_{B^0_s} \, [\,\mathrm{ps}\,]$	1.521 ± 0.005	1.521 ± 0.005

Table 5: Correlation matrix of the CP parameters and the external parameters from the decay-time fit to $B^0_s \to D^+_s D^-_s$.

	ϕ_s	$\lambda_{D^+_s D^-_s}$	Δm_s	$\Delta \Gamma_s$	$\tau_{B^0_s}$
ϕ_s	1.000	-0.007	-0.010	0.001	< 0.001
$\lambda_{D^+_s D^-_s}$		1.000	-0.018	-0.010	< 0.001
Δm_s			1.000	< 0.001	< 0.001
$\Delta \Gamma_s$				1.000	< 0.001
$\tau_{B^0_s}$					1.000

References

[1] R. Fleischer, *Exploring CP violation and penguin effects through $B_d^0 \to D^+D^-$ and $B_s^0 \to D_s^+D_s^-$*, Eur. Phys. J. **C51** (2007) 849, arXiv:0705.4421.

[2] R. Fleischer, *Extracting γ from $B_{s(d)} \to J/\psi K_S$ and $B_{d(s)} \to D_{d(s)}^+ D_{d(s)}^-$*, Eur. Phys. J. **C10** (1999) 299, arXiv:hep-ph/9903455.

[3] M. Jung and S. Schacht, *Standard model predictions and new physics sensitivity in $B \to DD$ decays*, Phys. Rev. **D91** (2015) 034027, arXiv:1410.8396.

[4] L. Bel *et al.*, *Anatomy of $B \to D\overline{D}$ decays*, JHEP **7** (2015) 108, arXiv:1505.01361.

[5] N. Cabibbo, *Unitary symmetry and leptonic decays*, Phys. Rev. Lett. **10** (1963) 531.

[6] M. Kobayashi and T. Maskawa, *CP-violation in the renormalizable theory of weak interaction*, Prog. Theor. Phys. **49** (1973) 652.

[7] LHCb collaboration, R. Aaij *et al.*, *Measurement of CP violation in $B^0 \to \psi(\to \ell^+\ell^-)K_S^0(\to \pi^+\pi^-)$ decays*, Phys. Rev. Lett. **132** (2024) 021801, arXiv:2309.09728.

[8] LHCb collaboration, R. Aaij *et al.*, *Measurement of CP violation in $B \to D^+D^-$ decays*, Phys. Rev. Lett. **117** (2016) 261801, arXiv:1608.06620.

[9] LHCb collaboration, R. Aaij *et al.*, *Measurement of the CP-violating phase ϕ_s in $\overline{B}_s^0 \to D_s^+D_s^-$ decays*, Phys. Rev. Lett. **113** (2014) 211801, arXiv:1409.4619.

[10] BaBar collaboration, B. Aubert *et al.*, *Measurements of time-dependent CP asymmetries in $B^0 \to D^{(*)+}D^{(*)-}$ decays*, Phys. Rev. **D79** (2009) 032002, arXiv:0808.1866.

[11] Belle collaboration, M. Röhrken *et al.*, *Measurements of branching fractions and time-dependent CP violating asymmetries in $B^0 \to D^{(*)\pm}D^{\mp}$ decays*, Phys. Rev. **D85** (2012) 091106, arXiv:1203.6647.

[12] LHCb collaboration, A. A. Alves Jr. *et al.*, *The LHCb detector at the LHC*, JINST **3** (2008) S08005.

[13] LHCb collaboration, R. Aaij *et al.*, *LHCb detector performance*, Int. J. Mod. Phys. **A30** (2015) 1530022, arXiv:1412.6352.

[14] R. Aaij *et al.*, *Performance of the LHCb Vertex Locator*, JINST **9** (2014) P09007, arXiv:1405.7808.

[15] P. d'Argent *et al.*, *Improved performance of the LHCb Outer Tracker in LHC Run 2*, JINST **12** (2017) P11016, arXiv:1708.00819.

[16] M. Adinolfi *et al.*, *Performance of the LHCb RICH detector at the LHC*, Eur. Phys. J. **C73** (2013) 2431, arXiv:1211.6759.

[17] A. A. Alves Jr. *et al.*, *Performance of the LHCb muon system*, JINST **8** (2013) P02022, arXiv:1211.1346.

[18] T. Sjöstrand, S. Mrenna, and P. Skands, *A brief introduction to PYTHIA 8.1*, Comput. Phys. Commun. **178** (2008) 852, arXiv:0710.3820; T. Sjöstrand, S. Mrenna, and P. Skands, *PYTHIA 6.4 physics and manual*, JHEP **05** (2006) 026, arXiv:hep-ph/0603175.

[19] I. Belyaev *et al.*, *Handling of the generation of primary events in Gauss, the LHCb simulation framework*, J. Phys. Conf. Ser. **331** (2011) 032047.

[20] D. J. Lange, *The EvtGen particle decay simulation package*, Nucl. Instrum. Meth. **A462** (2001) 152.

[21] N. Davidson, T. Przedzinski, and Z. Was, *PHOTOS interface in C++: Technical and physics documentation*, Comp. Phys. Comm. **199** (2016) 86, arXiv:1011.0937.

[22] Geant4 collaboration, J. Allison *et al.*, *Geant4 developments and applications*, IEEE Trans. Nucl. Sci. **53** (2006) 270; Geant4 collaboration, S. Agostinelli *et al.*, *Geant4: A simulation toolkit*, Nucl. Instrum. Meth. **A506** (2003) 250.

[23] M. Clemencic *et al.*, *The LHCb simulation application, Gauss: Design, evolution and experience*, J. Phys. Conf. Ser. **331** (2011) 032023.

[24] D. Müller, M. Clemencic, G. Corti, and M. Gersabeck, *ReDecay: A novel approach to speed up the simulation at LHCb*, Eur. Phys. J. **C78** (2018) 1009, arXiv:1810.10362.

[25] R. Aaij *et al.*, *Selection and processing of calibration samples to measure the particle identification performance of the LHCb experiment in Run 2*, Eur. Phys. J. Tech. Instr. **6** (2019) 1, arXiv:1803.00824.

[26] R. Aaij *et al.*, *The LHCb trigger and its performance in 2011*, JINST **8** (2013) P04022, arXiv:1211.3055.

[27] V. V. Gligorov and M. Williams, *Efficient, reliable and fast high-level triggering using a bonsai boosted decision tree*, JINST **8** (2013) P02013, arXiv:1210.6861.

[28] T. Likhomanenko *et al.*, *LHCb topological trigger reoptimization*, J. Phys. Conf. Ser. **664** (2015) 082025, arXiv:1510.00572.

[29] Particle Data Group, N. S. *et al.*, *Review of particle physics*, to be published in Phys. Rev **D110** (2024) 030001.

[30] F. Pedregosa *et al.*, *Scikit-learn: Machine learning in Python*, J. Machine Learning Res. **12** (2011) 2825, arXiv:1201.0490, and online at http://scikit-learn.org/stable/.

[31] A. Blum, A. Kalai, and J. Langford, *Beating the hold-out: bounds for k-fold and progressive cross-validation,* in *Proceedings of the Twelfth Annual Conference on Computational Learning Theory*, COLT '99, (New York, NY, USA), 203–208, Association for Computing Machinery, 1999.

[32] LHCb collaboration, R. Aaij *et al.*, *Measurement of the CP violating phase and decay-width difference in $B_s^0 \to \psi(2S)\phi$ decays*, Phys. Lett. **B762** (2016) 253, arXiv:1608.04855.

[33] W. D. Hulsbergen, *Decay chain fitting with a Kalman filter*, Nucl. Instrum. Meth. **A552** (2005) 566, arXiv:physics/0503191.

[34] M. Pivk and F. R. Le Diberder, *sPlot: A statistical tool to unfold data distributions*, Nucl. Instrum. Meth. **A555** (2005) 356, arXiv:physics/0402083.

[35] D. Martínez Santos and F. Dupertuis, *Mass distributions marginalized over per-event errors*, Nucl. Instrum. Meth. **A764** (2014) 150, arXiv:1312.5000.

[36] LHCb collaboration, R. Aaij *et al.*, *New algorithms for identifying the flavour of B^0 mesons using pions and protons*, Eur. Phys. J. **C77** (2017) 238, arXiv:1610.06019.

[37] LHCb collaboration, R. Aaij *et al.*, *A new algorithm for identifying the flavour of B_s^0 mesons at LHCb*, JINST **11** (2016) P05010, arXiv:1602.07252.

[38] LHCb collaboration, R. Aaij *et al.*, *Opposite-side flavour tagging of B mesons at the LHCb experiment*, Eur. Phys. J. **C72** (2012) 2022, arXiv:1202.4979.

[39] LHCb collaboration, R. Aaij *et al.*, *B flavour tagging using charm decays at the LHCb experiment*, JINST **10** (2015) P10005, arXiv:1507.07892.

[40] D. Fazzini, *Flavour Tagging in the LHCb experiment*, in *Proceedings, 6th Large Hadron Collider Physics Conference (LHCP 2018): Bologna, Italy, June 4-9, 2018*, **LHCP2018** 230, 2018.

[41] LHCb collaboration, R. Aaij *et al.*, *Measurements of the B^+, B^0, B_s^0 meson and Λ_b^0 baryon lifetimes*, JHEP **04** (2014) 114, arXiv:1402.2554.

[42] T. M. Karbach, G. Raven, and M. Schiller, *Decay time integrals in neutral meson mixing and their efficient evaluation*, arXiv:1407.0748.

[43] Particle Data Group, R. L. Workman *et al.*, *Review of particle physics*, Prog. Theor. Exp. Phys. **2022** (2022) 083C01.

[44] LHCb collaboration, R. Aaij *et al.*, *Measurement of CP violation in $B^0 \to D^{*\pm}D^{\mp}$ decays*, JHEP **03** (2020) 147, arXiv:1912.03723.

[45] LHCb collaboration, R. Aaij *et al.*, *Precise determination of the B_s^0-$\overline{B}_s^0$ oscillation frequency*, Nature Physics **18** (2022) 1, arXiv:2104.04421.

[46] B. Efron, *Bootstrap methods: Another look at the jackknife*, Ann. Statist. **7** (1979) 1.

[47] T. Skwarnicki, *A study of the radiative cascade transitions between the Upsilon-prime and Upsilon resonances*, PhD thesis, Institute of Nuclear Physics, Krakow, 1986, DESY-F31-86-02.

[48] S. S. Wilks, *The large-sample distribution of the likelihood ratio for testing composite hypotheses*, Ann. Math. Stat. **9** (1938) 60.

LHCb collaboration

R. Aaij[37] , A.S.W. Abdelmotteleb[56] , C. Abellan Beteta[50], F. Abudinén[56] ,
T. Ackernley[60] , A. A. Adefisoye[68] , B. Adeva[46] , M. Adinolfi[54] , P. Adlarson[81] ,
C. Agapopoulou[14] , C.A. Aidala[82] , Z. Ajaltouni[11], S. Akar[65] , K. Akiba[37] ,
P. Albicocco[27] , J. Albrecht[19] , F. Alessio[48] , M. Alexander[59] , Z. Aliouche[62] ,
P. Alvarez Cartelle[55] , R. Amalric[16] , S. Amato[3] , J.L. Amey[54] , Y. Amhis[14,48] ,
L. An[6] , L. Anderlini[26] , M. Andersson[50] , A. Andreianov[43] , P. Andreola[50] ,
M. Andreotti[25] , D. Andreou[68] , A. Anelli[30,n] , D. Ao[7] , F. Archilli[36,t] ,
M. Argenton[25] , S. Arguedas Cuendis[9,48] , A. Artamonov[43] , M. Artuso[68] ,
E. Aslanides[13] , R. Ataíde Da Silva[49] , M. Atzeni[64] , B. Audurier[12] , D. Bacher[63] ,
I. Bachiller Perea[10] , S. Bachmann[21] , M. Bachmayer[49] , J.J. Back[56] ,
P. Baladron Rodriguez[46] , V. Balagura[15] , W. Baldini[25] , L. Balzani[19] , H. Bao[7] ,
J. Baptista de Souza Leite[60] , C. Barbero Pretel[46,12] , M. Barbetti[26] , I. R. Barbosa[69] ,
R.J. Barlow[62] , M. Barnyakov[24] , S. Barsuk[14] , W. Barter[58] , M. Bartolini[55] ,
J. Bartz[68] , J.M. Basels[17] , S. Bashir[39] , G. Bassi[34,q] , B. Batsukh[5] , P. B. Battista[14],
A. Bay[49] , A. Beck[56] , M. Becker[19] , F. Bedeschi[34] , I.B. Bediaga[2] , N. A.
Behling[19] , S. Belin[46] , V. Bellee[50] , K. Belous[43] , I. Belov[28] , I. Belyaev[35] ,
G. Benane[13] , G. Bencivenni[27] , E. Ben-Haim[16] , A. Berezhnoy[43] , R. Bernet[50] ,
S. Bernet Andres[44] , A. Bertolin[32] , C. Betancourt[50] , F. Betti[58] , J. Bex[55] ,
Ia. Bezshyiko[50] , J. Bhom[40] , M.S. Bieker[19] , N.V. Biesuz[25] , P. Billoir[16] ,
A. Biolchini[37] , M. Birch[61] , F.C.R. Bishop[10] , A. Bitadze[62] , A. Bizzeti , T. Blake[56] ,
F. Blanc[49] , J.E. Blank[19] , S. Blusk[68] , V. Bocharnikov[43] , J.A. Boelhauve[19] ,
O. Boente Garcia[15] , T. Boettcher[65] , A. Bohare[58] , A. Boldyrev[43] , C.S. Bolognani[78] ,
R. Bolzonella[25,k] , N. Bondar[43] , A. Bordelius[48] , F. Borgato[32,o] , S. Borghi[62] ,
M. Borsato[30,n] , J.T. Borsuk[40] , S.A. Bouchiba[49] , M. Bovill[63] , T.J.V. Bowcock[60] ,
A. Boyer[48] , C. Bozzi[25] , A. Brea Rodriguez[49] , N. Breer[19] , J. Brodzicka[40] ,
A. Brossa Gonzalo[46,56,45,†] , J. Brown[60] , D. Brundu[31] , E. Buchanan[58], A. Buonaura[50] ,
L. Buonincontri[32,o] , A.T. Burke[62] , C. Burr[48] , J.S. Butter[55] , J. Buytaert[48] ,
W. Byczynski[48] , S. Cadeddu[31] , H. Cai[73], A. C. Caillet[16] , R. Calabrese[25,k] ,
S. Calderon Ramirez[9] , L. Calefice[45] , S. Cali[27] , M. Calvi[30,n] , M. Calvo Gomez[44] ,
P. Camargo Magalhaes[2,x] , J. I. Cambon Bouzas[46] , P. Campana[27] ,
D.H. Campora Perez[78] , A.F. Campoverde Quezada[7] , S. Capelli[30] , L. Capriotti[25] ,
R. Caravaca-Mora[9] , A. Carbone[24,i] , L. Carcedo Salgado[46] , R. Cardinale[28,l] ,
A. Cardini[31] , P. Carniti[30,n] , L. Carus[21], A. Casais Vidal[64] , R. Caspary[21] ,
G. Casse[60] , J. Castro Godinez[9] , M. Cattaneo[48] , G. Cavallero[25,48] , V. Cavallini[25,k] ,
S. Celani[21] , D. Cervenkov[63] , S. Cesare[29,m] , A.J. Chadwick[60] , I. Chahrour[82] ,
M. Charles[16] , Ph. Charpentier[48] , E. Chatzianagnostou[37] , M. Chefdeville[10] ,
C. Chen[13] , S. Chen[5] , Z. Chen[7] , A. Chernov[40] , S. Chernyshenko[52] , X.
Chiotopoulos[78] , V. Chobanova[80] , S. Cholak[49] , M. Chrzaszcz[40] , A. Chubykin[43] ,
V. Chulikov[43] , P. Ciambrone[27] , X. Cid Vidal[46] , G. Ciezarek[48] , P. Cifra[48] ,
P.E.L. Clarke[58] , M. Clemencic[48] , H.V. Cliff[55] , J. Closier[48] , C. Cocha Toapaxi[21] ,
V. Coco[48] , J. Cogan[13] , E. Cogneras[11] , L. Cojocariu[42] , P. Collins[48] ,
T. Colombo[48] , M. C. Colonna[19] , A. Comerma-Montells[45] , L. Congedo[23] ,
A. Contu[31] , N. Cooke[59] , I. Corredoira [46] , A. Correia[16] , G. Corti[48] ,
J.J. Cottee Meldrum[54], B. Couturier[48] , D.C. Craik[50] , M. Cruz Torres[2,f] ,
E. Curras Rivera[49] , R. Currie[58] , C.L. Da Silva[67] , S. Dadabaev[43] , L. Dai[70] ,
X. Dai[6] , E. Dall'Occo[19] , J. Dalseno[46] , C. D'Ambrosio[48] , J. Daniel[11] ,
A. Danilina[43] , P. d'Argent[23] , A. Davidson[56] , J.E. Davies[62] , A. Davis[62] ,
O. De Aguiar Francisco[62] , C. De Angelis[31,j] , F. De Benedetti[48] , J. de Boer[37] ,

K. De Bruyn[77] (ID), S. De Capua[62] (ID), M. De Cian[21,48] (ID), U. De Freitas Carneiro Da Graca[2,a] (ID),
E. De Lucia[27] (ID), J.M. De Miranda[2] (ID), L. De Paula[3] (ID), M. De Serio[23,g] (ID), P. De Simone[27] (ID),
F. De Vellis[19] (ID), J.A. de Vries[78] (ID), F. Debernardis[23] (ID), D. Decamp[10] (ID), V. Dedu[13] (ID), S.
Dekkers[1] (ID), L. Del Buono[16] (ID), B. Delaney[64] (ID), H.-P. Dembinski[19] (ID), J. Deng[8] (ID),
V. Denysenko[50] (ID), O. Deschamps[11] (ID), F. Dettori[31,j] (ID), B. Dey[76] (ID), P. Di Nezza[27] (ID),
I. Diachkov[43] (ID), S. Didenko[43] (ID), S. Ding[68] (ID), L. Dittmann[21] (ID), V. Dobishuk[52] (ID), A. D.
Docheva[59] (ID), C. Dong[4,b] (ID), A.M. Donohoe[22] (ID), F. Dordei[31] (ID), A.C. dos Reis[2] (ID), A. D.
Dowling[68] (ID), W. Duan[71] (ID), P. Duda[79] (ID), M.W. Dudek[40] (ID), L. Dufour[48] (ID), V. Duk[33] (ID),
P. Durante[48] (ID), M. M. Duras[79] (ID), J.M. Durham[67] (ID), O. D. Durmus[76] (ID), A. Dziurda[40] (ID),
A. Dzyuba[43] (ID), S. Easo[57] (ID), E. Eckstein[18], U. Egede[1] (ID), A. Egorychev[43] (ID), V. Egorychev[43] (ID),
S. Eisenhardt[58] (ID), E. Ejopu[62] (ID), L. Eklund[81] (ID), M. Elashri[65] (ID), J. Ellbracht[19] (ID), S. Ely[61] (ID),
A. Ene[42] (ID), E. Epple[65] (ID), J. Eschle[68] (ID), S. Esen[21] (ID), T. Evans[62] (ID), F. Fabiano[31,j] (ID),
L.N. Falcao[2] (ID), Y. Fan[7] (ID), B. Fang[73] (ID), L. Fantini[33,p,48] (ID), M. Faria[49] (ID), K. Farmer[58] (ID),
D. Fazzini[30,n] (ID), L. Felkowski[79] (ID), M. Feng[5,7] (ID), M. Feo[19,48] (ID), A. Fernandez Casani[47] (ID),
M. Fernandez Gomez[46] (ID), A.D. Fernez[66] (ID), F. Ferrari[24] (ID), F. Ferreira Rodrigues[3] (ID),
M. Ferrillo[50] (ID), M. Ferro-Luzzi[48] (ID), S. Filippov[43] (ID), R.A. Fini[23] (ID), M. Fiorini[25,k] (ID),
M. Firlej[39] (ID), K.L. Fischer[63] (ID), D.S. Fitzgerald[82] (ID), C. Fitzpatrick[62] (ID), T. Fiutowski[39] (ID),
F. Fleuret[15] (ID), M. Fontana[24] (ID), L. F. Foreman[62] (ID), R. Forty[48] (ID), D. Foulds-Holt[55] (ID),
V. Franco Lima[3] (ID), M. Franco Sevilla[66] (ID), M. Frank[48] (ID), E. Franzoso[25,k] (ID), G. Frau[62] (ID),
C. Frei[48] (ID), D.A. Friday[62] (ID), J. Fu[7] (ID), Q. Fuehring[19,55] (ID), Y. Fujii[1] (ID), T. Fulghesu[16] (ID),
E. Gabriel[37] (ID), G. Galati[23] (ID), M.D. Galati[37] (ID), A. Gallas Torreira[46] (ID), D. Galli[24,i] (ID),
S. Gambetta[58] (ID), M. Gandelman[3] (ID), P. Gandini[29] (ID), B. Ganie[62] (ID), H. Gao[7] (ID), R. Gao[63] (ID),
T.Q. Gao[55] (ID), Y. Gao[8] (ID), Y. Gao[6] (ID), Y. Gao[8], M. Garau[31,j] (ID), L.M. Garcia Martin[49] (ID),
P. Garcia Moreno[45] (ID), J. García Pardiñas[48] (ID), K. G. Garg[8] (ID), L. Garrido[45] (ID), C. Gaspar[48] (ID),
R.E. Geertsema[37] (ID), L.L. Gerken[19] (ID), E. Gersabeck[62] (ID), M. Gersabeck[62] (ID), T. Gershon[56] (ID),
S. G. Ghizzo[28,l], Z. Ghorbanimoghaddam[54], L. Giambastiani[32,o] (ID), F. I. Giasemis[16,e] (ID),
V. Gibson[55] (ID), H.K. Giemza[41] (ID), A.L. Gilman[63] (ID), M. Giovannetti[27] (ID), A. Gioventù[45] (ID),
L. Girardey[62] (ID), P. Gironella Gironell[45] (ID), C. Giugliano[25,k] (ID), M.A. Giza[40] (ID),
E.L. Gkougkousis[61] (ID), F.C. Glaser[14,21] (ID), V.V. Gligorov[16,48] (ID), C. Göbel[69] (ID),
E. Golobardes[44] (ID), D. Golubkov[43] (ID), A. Golutvin[61,43,48] (ID), S. Gomez Fernandez[45] (ID),
F. Goncalves Abrantes[63] (ID), M. Goncerz[40] (ID), G. Gong[4,b] (ID), J. A. Gooding[19] (ID),
I.V. Gorelov[43] (ID), C. Gotti[30] (ID), J.P. Grabowski[18] (ID), L.A. Granado Cardoso[48] (ID),
E. Graugés[45] (ID), E. Graverini[49,r] (ID), L. Grazette[56] (ID), G. Graziani (ID), A. T. Grecu[42] (ID),
L.M. Greeven[37] (ID), N.A. Grieser[65] (ID), L. Grillo[59] (ID), S. Gromov[43] (ID), C. Gu[15] (ID),
M. Guarise[25] (ID), L. Guerry[11] (ID), M. Guittiere[14] (ID), V. Guliaeva[43] (ID), P. A. Günther[21] (ID),
A.-K. Guseinov[49] (ID), E. Gushchin[43] (ID), Y. Guz[6,43,48] (ID), T. Gys[48] (ID), K. Habermann[18] (ID),
T. Hadavizadeh[1] (ID), C. Hadjivasiliou[66] (ID), G. Haefeli[49] (ID), C. Haen[48] (ID), J. Haimberger[48] (ID),
M. Hajheidari[48], G. Hallett[56] (ID), M.M. Halvorsen[48] (ID), P.M. Hamilton[66] (ID), J. Hammerich[60] (ID),
Q. Han[8] (ID), X. Han[21] (ID), S. Hansmann-Menzemer[21] (ID), L. Hao[7] (ID), N. Harnew[63] (ID),
M. Hartmann[14] (ID), S. Hashmi[39] (ID), J. He[7,c] (ID), F. Hemmer[48] (ID), C. Henderson[65] (ID),
R.D.L. Henderson[1,56] (ID), A.M. Hennequin[48] (ID), K. Hennessy[60] (ID), L. Henry[49] (ID), J. Herd[61] (ID),
P. Herrero Gascon[21] (ID), J. Heuel[17] (ID), A. Hicheur[3] (ID), G. Hijano Mendizabal[50], D. Hill[49] (ID),
S.E. Hollitt[19] (ID), J. Horswill[62] (ID), R. Hou[8] (ID), Y. Hou[11] (ID), N. Howarth[60], J. Hu[21], J. Hu[71] (ID),
W. Hu[6] (ID), X. Hu[4,b] (ID), W. Huang[7] (ID), W. Hulsbergen[37] (ID), R.J. Hunter[56] (ID), M. Hushchyn[43] (ID),
D. Hutchcroft[60] (ID), M. Idzik[39] (ID), D. Ilin[43] (ID), P. Ilten[65] (ID), A. Inglessi[43] (ID), A. Iniukhin[43] (ID),
A. Ishteev[43] (ID), K. Ivshin[43] (ID), R. Jacobsson[48] (ID), H. Jage[17] (ID), S.J. Jaimes Elles[47,74] (ID),
S. Jakobsen[48] (ID), E. Jans[37] (ID), B.K. Jashal[47] (ID), A. Jawahery[66,48] (ID), V. Jevtic[19] (ID),
E. Jiang[66] (ID), X. Jiang[5,7] (ID), Y. Jiang[7] (ID), Y. J. Jiang[6] (ID), M. John[63] (ID), A.
John Rubesh Rajan[22] (ID), D. Johnson[53] (ID), C.R. Jones[55] (ID), T.P. Jones[56] (ID), S. Joshi[41] (ID),
B. Jost[48] (ID), J. Juan Castella[55] (ID), N. Jurik[48] (ID), I. Juszczak[40] (ID), D. Kaminaris[49] (ID),

S. Kandybei[51], M. Kane[58], Y. Kang[4,b], C. Kar[11], M. Karacson[48],
D. Karpenkov[43], A. Kauniskangas[49], J.W. Kautz[65], M.K. Kazanecki[40], F. Keizer[48],
M. Kenzie[55], T. Ketel[37], B. Khanji[68], A. Kharisova[43], S. Kholodenko[34,48],
G. Khreich[14], T. Kirn[17], V.S. Kirsebom[30,n], O. Kitouni[64], S. Klaver[38],
N. Kleijne[34,q], K. Klimaszewski[41], M.R. Kmiec[41], S. Koliiev[52], L. Kolk[19],
A. Konoplyannikov[43], P. Kopciewicz[39,48], P. Koppenburg[37], M. Korolev[43],
I. Kostiuk[37], O. Kot[52], S. Kotriakhova, A. Kozachuk[43], P. Kravchenko[43],
L. Kravchuk[43], M. Kreps[56], P. Krokovny[43], W. Krupa[68], W. Krzemien[41],
O.K. Kshyvanskyi[52], S. Kubis[79], M. Kucharczyk[40], V. Kudryavtsev[43], E. Kulikova[43],
A. Kupsc[81], B. K. Kutsenko[13], D. Lacarrere[48], P. Laguarta Gonzalez[45], A. Lai[31],
A. Lampis[31], D. Lancierini[55], C. Landesa Gomez[46], J.J. Lane[1], R. Lane[54],
G. Lanfranchi[27], C. Langenbruch[21], J. Langer[19], O. Lantwin[43], T. Latham[56],
F. Lazzari[34,r], C. Lazzeroni[53], R. Le Gac[13], H. Lee[60], R. Lefèvre[11], A. Leflat[43],
S. Legotin[43], M. Lehuraux[56], E. Lemos Cid[48], O. Leroy[13], T. Lesiak[40], E. Lesser[48],
B. Leverington[21], A. Li[4,b], C. Li[13], H. Li[71], K. Li[8], L. Li[62], M. Li[8], P. Li[7],
P.-R. Li[72], Q. Li[5,7], S. Li[8], T. Li[5,d], T. Li[71], Y. Li[8], Y. Li[5], Z. Lian[4,b],
X. Liang[68], S. Libralon[47], C. Lin[7], T. Lin[57], R. Lindner[48], V. Lisovskyi[49],
R. Litvinov[31,48], F. L. Liu[1], G. Liu[71], K. Liu[72], S. Liu[5,7], W. Liu[8], Y. Liu[58],
Y. Liu[72], Y. L. Liu[61], A. Lobo Salvia[45], A. Loi[31], J. Lomba Castro[46], T. Long[55],
J.H. Lopes[3], A. Lopez Huertas[45], S. López Soliño[46], Q. Lu[15], C. Lucarelli[26],
D. Lucchesi[32,o], M. Lucio Martinez[78], V. Lukashenko[37,52], Y. Luo[6], A. Lupato[32,h],
E. Luppi[25,k], K. Lynch[22], X.-R. Lyu[7], G. M. Ma[4,b], R. Ma[7], S. Maccolini[19],
F. Machefert[14], F. Maciuc[42], B. Mack[68], I. Mackay[63], L. M. Mackey[68],
L.R. Madhan Mohan[55], M. J. Madurai[53], A. Maevskiy[43], D. Magdalinski[37],
D. Maisuzenko[43], M.W. Majewski[39], J.J. Malczewski[40], S. Malde[63], L. Malentacca[48],
A. Malinin[43], T. Maltsev[43], G. Manca[31,j], G. Mancinelli[13], C. Mancuso[29,14,m],
R. Manera Escalero[45], D. Manuzzi[24], D. Marangotto[29,m], J.F. Marchand[10],
R. Marchevski[49], U. Marconi[24], E. Mariani[16], S. Mariani[48], C. Marin Benito[45],
J. Marks[21], A.M. Marshall[54], L. Martel[63], G. Martelli[33,p], G. Martellotti[35],
L. Martinazzoli[48], M. Martinelli[30,n], D. Martinez Santos[46], F. Martinez Vidal[47],
A. Massafferri[2], R. Matev[48], A. Mathad[48], V. Matiunin[43], C. Matteuzzi[68],
K.R. Mattioli[15], A. Mauri[61], E. Maurice[15], J. Mauricio[45], P. Mayencourt[49],
J. Mazorra de Cos[47], M. Mazurek[41], M. McCann[61], L. Mcconnell[22],
T.H. McGrath[62], N.T. McHugh[59], A. McNab[62], R. McNulty[22], B. Meadows[65],
G. Meier[19], D. Melnychuk[41], F. M. Meng[4,b], M. Merk[37,78], A. Merli[49],
L. Meyer Garcia[66], D. Miao[5,7], H. Miao[7], M. Mikhasenko[75], D.A. Milanes[74],
A. Minotti[30,n], E. Minucci[68], T. Miralles[11], B. Mitreska[19], D.S. Mitzel[19],
A. Modak[57], R.A. Mohammed[63], R.D. Moise[17], S. Mokhnenko[43], E.
F. Molina Cardenas[82], T. Mombächer[48], M. Monk[56,1], S. Monteil[11],
A. Morcillo Gomez[46], G. Morello[27], M.J. Morello[34,q], M.P. Morgenthaler[21],
J. Moron[39], A.B. Morris[48], A.G. Morris[13], R. Mountain[68], H. Mu[4,b], Z. M. Mu[6],
E. Muhammad[56], F. Muheim[58], M. Mulder[77], K. Müller[50], F. Muñoz-Rojas[9],
R. Murta[61], P. Naik[60], T. Nakada[49], R. Nandakumar[57], T. Nanut[48], I. Nasteva[3],
M. Needham[58], N. Neri[29,m], S. Neubert[18], N. Neufeld[48], P. Neustroev[43],
J. Nicolini[19,14], D. Nicotra[78], E.M. Niel[49], N. Nikitin[43], P. Nogarolli[3], P. Nogga[18],
C. Normand[54], J. Novoa Fernandez[46], G. Nowak[65], C. Nunez[82], H. N. Nur[59],
A. Oblakowska-Mucha[39], V. Obraztsov[43], T. Oeser[17], S. Okamura[25,k],
A. Okhotnikov[43], O. Okhrimenko[52], R. Oldeman[31,j], F. Oliva[58], M. Olocco[19],
C.J.G. Onderwater[78], R.H. O'Neil[58], D. Osthues[19], J.M. Otalora Goicochea[3],
P. Owen[50], A. Oyanguren[47], O. Ozcelik[58], F. Paciolla[34,u], A. Padee[41],

K.O. Padeken[18] , B. Pagare[56] , P.R. Pais[21] , T. Pajero[48] , A. Palano[23] ,
M. Palutan[27] , G. Panshin[43] , L. Paolucci[56] , A. Papanestis[57,48] , M. Pappagallo[23,g] ,
L.L. Pappalardo[25,k] , C. Pappenheimer[65] , C. Parkes[62] , B. Passalacqua[25] ,
G. Passaleva[26] , D. Passaro[34,q] , A. Pastore[23] , M. Patel[61] , J. Patoc[63] ,
C. Patrignani[24,i] , A. Paul[68] , C.J. Pawley[78] , A. Pellegrino[37] , J. Peng[5,7] ,
M. Pepe Altarelli[27] , S. Perazzini[24] , D. Pereima[43] , H. Pereira Da Costa[67] ,
A. Pereiro Castro[46] , P. Perret[11] , A. Perro[48] , K. Petridis[54] , A. Petrolini[28,l] , J. P.
Pfaller[65] , H. Pham[68] , L. Pica[34,q] , M. Piccini[33] , L. Piccolo[31] , B. Pietrzyk[10] ,
G. Pietrzyk[14] , D. Pinci[35] , F. Pisani[48] , M. Pizzichemi[30,n,48] , V. Placinta[42] ,
M. Plo Casasus[46] , T. Poeschl[48] , F. Polci[16,48] , M. Poli Lener[27] , A. Poluektov[13] ,
N. Polukhina[43] , I. Polyakov[43] , E. Polycarpo[3] , S. Ponce[48] , D. Popov[7] ,
S. Poslavskii[43] , K. Prasanth[58] , C. Prouve[46] , D. Provenzano[31,j] , V. Pugatch[52] ,
G. Punzi[34,r] , S. Qasim[50] , Q. Q. Qian[6] , W. Qian[7] , N. Qin[4,b] , S. Qu[4,b] ,
R. Quagliani[48] , R.I. Rabadan Trejo[56] , J.H. Rademacker[54] , M. Rama[34] , M.
Ramírez García[82] , V. Ramos De Oliveira[69] , M. Ramos Pernas[56] , M.S. Rangel[3] ,
F. Ratnikov[43] , G. Raven[38] , M. Rebollo De Miguel[47] , F. Redi[29,h] , J. Reich[54] ,
F. Reiss[62] , Z. Ren[7] , P.K. Resmi[63] , R. Ribatti[49] , G. R. Ricart[15,12] ,
D. Riccardi[34,q] , S. Ricciardi[57] , K. Richardson[64] , M. Richardson-Slipper[58] ,
K. Rinnert[60] , P. Robbe[14] , G. Robertson[59] , E. Rodrigues[60] ,
E. Rodriguez Fernandez[46] , J.A. Rodriguez Lopez[74] , E. Rodriguez Rodriguez[46] ,
J. Roensch[19] , A. Rogachev[43] , A. Rogovskiy[57] , D.L. Rolf[48] , P. Roloff[48] ,
V. Romanovskiy[65] , M. Romero Lamas[46] , A. Romero Vidal[46] , G. Romolini[25] ,
F. Ronchetti[49] , T. Rong[6] , M. Rotondo[27] , S. R. Roy[21] , M.S. Rudolph[68] ,
M. Ruiz Diaz[21] , R.A. Ruiz Fernandez[46] , J. Ruiz Vidal[81,y] , A. Ryzhikov[43] ,
J. Ryzka[39] , J. J. Saavedra-Arias[9] , J.J. Saborido Silva[46] , R. Sadek[15] , N. Sagidova[43] ,
D. Sahoo[76] , N. Sahoo[53] , B. Saitta[31,j] , M. Salomoni[30,n,48] , I. Sanderswood[47] ,
R. Santacesaria[35] , C. Santamarina Rios[46] , M. Santimaria[27,48] , L. Santoro [2] ,
E. Santovetti[36] , A. Saputi[25,48] , D. Saranin[43] , A. Sarnatskiy[77] , G. Sarpis[58] ,
M. Sarpis[62] , C. Satriano[35,s] , A. Satta[36] , M. Saur[6] , D. Savrina[43] , H. Sazak[17] ,
F. Sborzacchi[48,27] , L.G. Scantlebury Smead[63] , A. Scarabotto[19] , S. Schael[17] ,
S. Scherl[60] , M. Schiller[59] , H. Schindler[48] , M. Schmelling[20] , B. Schmidt[48] ,
S. Schmitt[17] , H. Schmitz[18], O. Schneider[49] , A. Schopper[48] , N. Schulte[19] ,
S. Schulte[49] , M.H. Schune[14] , R. Schwemmer[48] , G. Schwering[17] , B. Sciascia[27] ,
A. Sciuccati[48] , S. Sellam[46] , A. Semennikov[43] , T. Senger[50] , M. Senghi Soares[38] ,
A. Sergi[28,l,48] , N. Serra[50] , L. Sestini[32] , A. Seuthe[19] , Y. Shang[6] , D.M. Shangase[82] ,
M. Shapkin[43] , R. S. Sharma[68] , I. Shchemerov[43] , L. Shchutska[49] , T. Shears[60] ,
L. Shekhtman[43] , Z. Shen[6] , S. Sheng[5,7] , V. Shevchenko[43] , B. Shi[7] , Q. Shi[7] ,
Y. Shimizu[14] , E. Shmanin[24] , R. Shorkin[43] , J.D. Shupperd[68] , R. Silva Coutinho[68] ,
G. Simi[32,o] , S. Simone[23,g] , N. Skidmore[56] , T. Skwarnicki[68] , M.W. Slater[53] ,
J.C. Smallwood[63] , E. Smith[64] , K. Smith[67] , M. Smith[61] , A. Snoch[37] ,
L. Soares Lavra[58] , M.D. Sokoloff[65] , F.J.P. Soler[59] , A. Solomin[43,54] , A. Solovev[43] ,
I. Solovyev[43] , R. Song[1] , Y. Song[49] , Y. Song[4,b] , Y. S. Song[6] ,
F.L. Souza De Almeida[68] , B. Souza De Paula[3] , E. Spadaro Norella[28,l] , E. Spedicato[24] ,
J.G. Speer[19] , E. Spiridenkov[43] , P. Spradlin[59] , V. Sriskaran[48] , F. Stagni[48] ,
M. Stahl[48] , S. Stahl[48] , S. Stanislaus[63] , E.N. Stein[48] , O. Steinkamp[50] ,
O. Stenyakin[43] , H. Stevens[19] , D. Strekalina[43] , Y. Su[7] , F. Suljik[63] , J. Sun[31] ,
L. Sun[73] , Y. Sun[66] , D. Sundfeld[2] , W. Sutcliffe[50] , P.N. Swallow[53] , K. Swientek[39] ,
F. Swystun[55] , A. Szabelski[41] , T. Szumlak[39] , Y. Tan[4,b] , M.D. Tat[63] ,
A. Terentev[43] , F. Terzuoli[34,u,48] , F. Teubert[48] , E. Thomas[48] , D.J.D. Thompson[53] ,
H. Tilquin[61] , V. Tisserand[11] , S. T'Jampens[10] , M. Tobin[5,48] , L. Tomassetti[25,k] ,

G. Tonani[29,m,48] , X. Tong[6] , D. Torres Machado[2] , L. Toscano[19] , D.Y. Tou[4,b] ,
C. Trippl[44] , G. Tuci[21] , N. Tuning[37] , L.H. Uecker[21] , A. Ukleja[39] ,
D.J. Unverzagt[21] , E. Ursov[43] , A. Usachov[38] , A. Ustyuzhanin[43] , U. Uwer[21] ,
V. Vagnoni[24] , V. Valcarce Cadenas[46] , G. Valenti[24] , N. Valls Canudas[48] ,
H. Van Hecke[67] , E. van Herwijnen[61] , C.B. Van Hulse[46,w] , R. Van Laak[49] ,
M. van Veghel[37] , G. Vasquez[50] , R. Vazquez Gomez[45] , P. Vazquez Regueiro[46] ,
C. Vázquez Sierra[46] , S. Vecchi[25] , J.J. Velthuis[54] , M. Veltri[26,v] , A. Venkateswaran[49] ,
M. Verdoglia[31] , M. Vesterinen[56] , D. Vico Benet[63] , P. V. Vidrier Villalba[45],
M. Vieites Diaz[48] , X. Vilasis-Cardona[44] , E. Vilella Figueras[60] , A. Villa[24] ,
P. Vincent[16] , F.C. Volle[53] , D. vom Bruch[13] , N. Voropaev[43] , K. Vos[78] ,
G. Vouters[10] , C. Vrahas[58] , J. Wagner[19] , J. Walsh[34] , E.J. Walton[1,56] , G. Wan[6] ,
C. Wang[21] , G. Wang[8] , J. Wang[6] , J. Wang[5] , J. Wang[4,b] , J. Wang[73] ,
M. Wang[29] , N. W. Wang[7] , R. Wang[54] , X. Wang[8] , X. Wang[71] , X. W. Wang[61] ,
Y. Wang[6] , Z. Wang[14] , Z. Wang[4,b] , Z. Wang[29] , J.A. Ward[56,1] , M. Waterlaat[48],
N.K. Watson[53] , D. Websdale[61] , Y. Wei[6] , J. Wendel[80] , B.D.C. Westhenry[54] ,
C. White[55] , M. Whitehead[59] , E. Whiter[53] , A.R. Wiederhold[62] , D. Wiedner[19] ,
G. Wilkinson[63] , M.K. Wilkinson[65] , M. Williams[64] , M.R.J. Williams[58] ,
R. Williams[55] , Z. Williams[54] , F.F. Wilson[57] , M. Winn[12] , W. Wislicki[41] ,
M. Witek[40] , L. Witola[21] , G. Wormser[14] , S.A. Wotton[55] , H. Wu[68] , J. Wu[8] ,
Y. Wu[6] , Z. Wu[7] , K. Wyllie[48] , S. Xian[71] , Z. Xiang[5] , Y. Xie[8] , A. Xu[34] , J. Xu[7] ,
L. Xu[4,b] , L. Xu[4,b] , M. Xu[56] , Z. Xu[48] , Z. Xu[7] , Z. Xu[5] , D. Yang[4] , K. Yang[61] ,
S. Yang[7] , X. Yang[6] , Y. Yang[28,l] , Z. Yang[6] , Z. Yang[66] , V. Yeroshenko[14] ,
H. Yeung[62] , H. Yin[8] , C. Y. Yu[6] , J. Yu[70] , X. Yuan[5] , Y Yuan[5,7] ,
E. Zaffaroni[49] , M. Zavertyaev[20] , M. Zdybal[40] , F. Zenesini[24,i] , C. Zeng[5,7] ,
M. Zeng[4,b] , C. Zhang[6] , D. Zhang[8] , J. Zhang[7] , L. Zhang[4,b] , S. Zhang[70] ,
S. Zhang[63] , Y. Zhang[6] , Y. Z. Zhang[4,b] , Y. Zhao[21] , A. Zharkova[43] ,
A. Zhelezov[21] , S. Z. Zheng[6] , X. Z. Zheng[4,b] , Y. Zheng[7] , T. Zhou[6] , X. Zhou[8] ,
Y. Zhou[7] , V. Zhovkovska[56] , L. Z. Zhu[7] , X. Zhu[4,b] , X. Zhu[8] , V. Zhukov[17] ,
J. Zhuo[47] , Q. Zou[5,7] , D. Zuliani[32,o] , G. Zunica[49] .

[1] School of Physics and Astronomy, Monash University, Melbourne, Australia
[2] Centro Brasileiro de Pesquisas Físicas (CBPF), Rio de Janeiro, Brazil
[3] Universidade Federal do Rio de Janeiro (UFRJ), Rio de Janeiro, Brazil
[4] Department of Engineering Physics, Tsinghua University, Beijing, China, Beijing, China
[5] Institute Of High Energy Physics (IHEP), Beijing, China
[6] School of Physics State Key Laboratory of Nuclear Physics and Technology, Peking University, Beijing, China
[7] University of Chinese Academy of Sciences, Beijing, China
[8] Institute of Particle Physics, Central China Normal University, Wuhan, Hubei, China
[9] Consejo Nacional de Rectores (CONARE), San Jose, Costa Rica
[10] Université Savoie Mont Blanc, CNRS, IN2P3-LAPP, Annecy, France
[11] Université Clermont Auvergne, CNRS/IN2P3, LPC, Clermont-Ferrand, France
[12] Département de Physique Nucléaire (DPhN), Gif-Sur-Yvette, France
[13] Aix Marseille Univ, CNRS/IN2P3, CPPM, Marseille, France
[14] Université Paris-Saclay, CNRS/IN2P3, IJCLab, Orsay, France
[15] Laboratoire Leprince-Ringuet, CNRS/IN2P3, Ecole Polytechnique, Institut Polytechnique de Paris, Palaiseau, France
[16] LPNHE, Sorbonne Université, Paris Diderot Sorbonne Paris Cité, CNRS/IN2P3, Paris, France
[17] I. Physikalisches Institut, RWTH Aachen University, Aachen, Germany
[18] Universität Bonn - Helmholtz-Institut für Strahlen und Kernphysik, Bonn, Germany
[19] Fakultät Physik, Technische Universität Dortmund, Dortmund, Germany
[20] Max-Planck-Institut für Kernphysik (MPIK), Heidelberg, Germany
[21] Physikalisches Institut, Ruprecht-Karls-Universität Heidelberg, Heidelberg, Germany

[22] School of Physics, University College Dublin, Dublin, Ireland
[23] INFN Sezione di Bari, Bari, Italy
[24] INFN Sezione di Bologna, Bologna, Italy
[25] INFN Sezione di Ferrara, Ferrara, Italy
[26] INFN Sezione di Firenze, Firenze, Italy
[27] INFN Laboratori Nazionali di Frascati, Frascati, Italy
[28] INFN Sezione di Genova, Genova, Italy
[29] INFN Sezione di Milano, Milano, Italy
[30] INFN Sezione di Milano-Bicocca, Milano, Italy
[31] INFN Sezione di Cagliari, Monserrato, Italy
[32] INFN Sezione di Padova, Padova, Italy
[33] INFN Sezione di Perugia, Perugia, Italy
[34] INFN Sezione di Pisa, Pisa, Italy
[35] INFN Sezione di Roma La Sapienza, Roma, Italy
[36] INFN Sezione di Roma Tor Vergata, Roma, Italy
[37] Nikhef National Institute for Subatomic Physics, Amsterdam, Netherlands
[38] Nikhef National Institute for Subatomic Physics and VU University Amsterdam, Amsterdam, Netherlands
[39] AGH - University of Krakow, Faculty of Physics and Applied Computer Science, Kraków, Poland
[40] Henryk Niewodniczanski Institute of Nuclear Physics Polish Academy of Sciences, Kraków, Poland
[41] National Center for Nuclear Research (NCBJ), Warsaw, Poland
[42] Horia Hulubei National Institute of Physics and Nuclear Engineering, Bucharest-Magurele, Romania
[43] Affiliated with an institute covered by a cooperation agreement with CERN
[44] DS4DS, La Salle, Universitat Ramon Llull, Barcelona, Spain
[45] ICCUB, Universitat de Barcelona, Barcelona, Spain
[46] Instituto Galego de Física de Altas Enerxías (IGFAE), Universidade de Santiago de Compostela, Santiago de Compostela, Spain
[47] Instituto de Fisica Corpuscular, Centro Mixto Universidad de Valencia - CSIC, Valencia, Spain
[48] European Organization for Nuclear Research (CERN), Geneva, Switzerland
[49] Institute of Physics, Ecole Polytechnique Fédérale de Lausanne (EPFL), Lausanne, Switzerland
[50] Physik-Institut, Universität Zürich, Zürich, Switzerland
[51] NSC Kharkiv Institute of Physics and Technology (NSC KIPT), Kharkiv, Ukraine
[52] Institute for Nuclear Research of the National Academy of Sciences (KINR), Kyiv, Ukraine
[53] School of Physics and Astronomy, University of Birmingham, Birmingham, United Kingdom
[54] H.H. Wills Physics Laboratory, University of Bristol, Bristol, United Kingdom
[55] Cavendish Laboratory, University of Cambridge, Cambridge, United Kingdom
[56] Department of Physics, University of Warwick, Coventry, United Kingdom
[57] STFC Rutherford Appleton Laboratory, Didcot, United Kingdom
[58] School of Physics and Astronomy, University of Edinburgh, Edinburgh, United Kingdom
[59] School of Physics and Astronomy, University of Glasgow, Glasgow, United Kingdom
[60] Oliver Lodge Laboratory, University of Liverpool, Liverpool, United Kingdom
[61] Imperial College London, London, United Kingdom
[62] Department of Physics and Astronomy, University of Manchester, Manchester, United Kingdom
[63] Department of Physics, University of Oxford, Oxford, United Kingdom
[64] Massachusetts Institute of Technology, Cambridge, MA, United States
[65] University of Cincinnati, Cincinnati, OH, United States
[66] University of Maryland, College Park, MD, United States
[67] Los Alamos National Laboratory (LANL), Los Alamos, NM, United States
[68] Syracuse University, Syracuse, NY, United States
[69] Pontifícia Universidade Católica do Rio de Janeiro (PUC-Rio), Rio de Janeiro, Brazil, associated to [3]
[70] School of Physics and Electronics, Hunan University, Changsha City, China, associated to [8]
[71] Guangdong Provincial Key Laboratory of Nuclear Science, Guangdong-Hong Kong Joint Laboratory of Quantum Matter, Institute of Quantum Matter, South China Normal University, Guangzhou, China, associated to [4]
[72] Lanzhou University, Lanzhou, China, associated to [5]
[73] School of Physics and Technology, Wuhan University, Wuhan, China, associated to [4]

[74] *Departamento de Fisica , Universidad Nacional de Colombia, Bogota, Colombia, associated to* [16]

[75] *Ruhr Universitaet Bochum, Fakultaet f. Physik und Astronomie, Bochum, Germany, associated to* [19]

[76] *Eotvos Lorand University, Budapest, Hungary, associated to* [48]

[77] *Van Swinderen Institute, University of Groningen, Groningen, Netherlands, associated to* [37]

[78] *Universiteit Maastricht, Maastricht, Netherlands, associated to* [37]

[79] *Tadeusz Kosciuszko Cracow University of Technology, Cracow, Poland, associated to* [40]

[80] *Universidade da Coruña, A Coruna, Spain, associated to* [44]

[81] *Department of Physics and Astronomy, Uppsala University, Uppsala, Sweden, associated to* [59]

[82] *University of Michigan, Ann Arbor, MI, United States, associated to* [68]

[a] *Centro Federal de Educacão Tecnológica Celso Suckow da Fonseca, Rio De Janeiro, Brazil*

[b] *Center for High Energy Physics, Tsinghua University, Beijing, China*

[c] *Hangzhou Institute for Advanced Study, UCAS, Hangzhou, China*

[d] *School of Physics and Electronics, Henan University , Kaifeng, China*

[e] *LIP6, Sorbonne Université, Paris, France*

[f] *Universidad Nacional Autónoma de Honduras, Tegucigalpa, Honduras*

[g] *Università di Bari, Bari, Italy*

[h] *Università di Bergamo, Bergamo, Italy*

[i] *Università di Bologna, Bologna, Italy*

[j] *Università di Cagliari, Cagliari, Italy*

[k] *Università di Ferrara, Ferrara, Italy*

[l] *Università di Genova, Genova, Italy*

[m] *Università degli Studi di Milano, Milano, Italy*

[n] *Università degli Studi di Milano-Bicocca, Milano, Italy*

[o] *Università di Padova, Padova, Italy*

[p] *Università di Perugia, Perugia, Italy*

[q] *Scuola Normale Superiore, Pisa, Italy*

[r] *Università di Pisa, Pisa, Italy*

[s] *Università della Basilicata, Potenza, Italy*

[t] *Università di Roma Tor Vergata, Roma, Italy*

[u] *Università di Siena, Siena, Italy*

[v] *Università di Urbino, Urbino, Italy*

[w] *Universidad de Alcalá, Alcalá de Henares , Spain*

[x] *Facultad de Ciencias Fisicas, Madrid, Spain*

[y] *Department of Physics/Division of Particle Physics, Lund, Sweden*

[†] *Deceased*